

# Impact of Kinetic Models on Methanol Synthesis Reactor Predictions: In Silico Assessment and Comparison with Industrial Data

Filippo Bisotti, Matteo Fedeli, Kristiano Prifti, Andrea Galeazzi, Anna Dell'Angelo, and Flavio Manenti\*



Cite This: *Ind. Eng. Chem. Res.* 2022, 61, 2206–2226

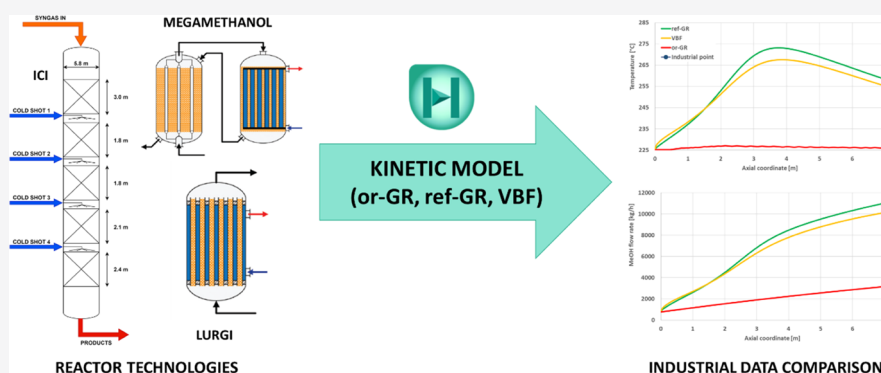


Read Online

ACCESS |

Metrics & More

Article Recommendations



**ABSTRACT:** The reactor is one of the most important equipment to be designed for optimal process operations. An appropriate reactor modeling leads to an efficient and optimal process conceptual design, simulation, and eventually construction. The key for success in this step is mainly related to kinetics. The present work is centered toward process simulation and aims at comparing three different kinetic models for methanol synthesis. The comparison shows how the refitted Graaf model, presented in a previous study, effectively predicts the performance of modern methanol synthesis loops. To pursue this objective, we simulated in Aspen HYSYS three methanol synthesis technologies (the most popular technologies in modern plants) and compared the results with industrial data. The proposed case study demonstrates that the refitted Graaf model is more accurate in output prediction than the well-established original Graaf and Vanden Bussche–Froment models, which are currently considered the industrial benchmark, thus showing how the refitted Graaf model is a potential candidate for future industrial applications.

## INTRODUCTION—A BRIEF INTRODUCTION ON THE METHANOL SYNTHESIS KINETICS AND REACTOR TECHNOLOGIES

It is well known that an appropriate thermodynamic toolbox selection benefits the accuracy and reliability of the process design.<sup>1–3</sup> This step also positively influences the process optimization and control.<sup>4–6</sup> Similarly, an accurate kinetic model enables us to properly configure and define the downstream for the product purification. This leads to savings in energy and volumes while also reducing the uncertainty in the reactor design and in the overall methanol plant design.<sup>7,8</sup> More in general, several recent works highlight how accurate kinetics are crucial for highly intensified processes.<sup>9–12</sup>

This premise is considering the trends in the methanol sector in terms of production volumes, energy consumption, and future perspectives.<sup>13</sup> In the last decades, the methanol molecule has gained increasing interest thanks to its peculiar features, which make it an appealing alternative fuel and hydrogen vector for energy transition.<sup>14–16</sup> Moreover, patent-

filing trends and the production volume outlooks have witnessed growing interest around methanol manufacturing as mentioned in Olah's Methanol Economy Project. More in general, methanol production is playing a dominant role in the decarbonization process and net-zero emissions target. It is important to remark that CO<sub>2</sub> capture and storage (CCS) through compression (possibly liquefaction) and storage is a costly alternative, which is unavoidable for production sites that are very isolated (i.e., off-shore platform) or not well integrated in a production network.<sup>17,18</sup> Recently, CO<sub>2</sub> utilization (CU) is making CCS systems more economically appealing. Indeed, both CCS and CU are economically

**Received:** November 17, 2021

**Revised:** January 14, 2022

**Accepted:** January 19, 2022

**Published:** January 31, 2022

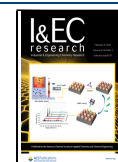


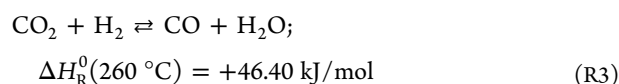
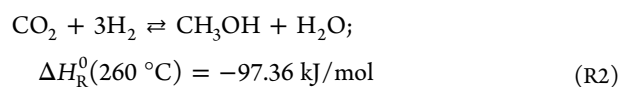
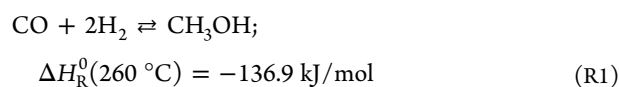
Table 1. Kinetic Models Including Works Dealing with Kinetic Parameters Refit

model	carbon source	reactions	notes
Villa et al. <sup>32</sup>	CO	CO + 2H <sub>2</sub> ⇌ CH <sub>3</sub> OH CO <sub>2</sub> + H <sub>2</sub> ⇌ CO + H <sub>2</sub> O	CO <sub>2</sub> direct hydrogenation not considered
Klier et al. <sup>33</sup> McNeil et al. <sup>48</sup> Ma et al. <sup>49</sup>		CO + 2H <sub>2</sub> ⇌ CH <sub>3</sub> OH CO <sub>2</sub> + 3H <sub>2</sub> ⇌ CH <sub>3</sub> OH + H <sub>2</sub> O	RWGS does not occurs on the catalyst
Takagawa et al. <sup>50</sup> Graaf et al. <sup>51</sup> Lim et al. <sup>36</sup> Park et al. <sup>35</sup> Seidel et al. <sup>34</sup> Nestler et al. <sup>52</sup> Slotboom et al. <sup>44</sup> Lacerda de Oliveira Campos et al. <sup>43</sup> Bisotti et al. <sup>13</sup>	CO and CO <sub>2</sub>	CO + 2H <sub>2</sub> ⇌ CH <sub>3</sub> OH CO <sub>2</sub> + 3H <sub>2</sub> ⇌ CH <sub>3</sub> OH + H <sub>2</sub> O CO <sub>2</sub> + H <sub>2</sub> ⇌ CO + H <sub>2</sub> O	complete scheme
Skrzypek et al. <sup>53</sup> Askgaard et al. <sup>54</sup> Vanden Bussche–Froment <sup>55</sup> Kubota et al. <sup>56</sup>	CO <sub>2</sub>	CO <sub>2</sub> + 3H <sub>2</sub> ⇌ CH <sub>3</sub> OH + H <sub>2</sub> O CO <sub>2</sub> + H <sub>2</sub> ⇌ CO + H <sub>2</sub> O	CO direct hydrogenation is removed

expensive, but their synergy and coupling lead to new promising frontiers to mitigate and possibly solve the CO<sub>2</sub> problem. This is mainly due to the possibility to produce valuable chemicals starting from waste such as carbon dioxide. Hence, carbon capture and utilization (CCU) enables us to increase the overall process profitability by reducing the greenhouse gas emission.<sup>19–23</sup> Not surprisingly, many research activities are devoted to directly exploit CO<sub>2</sub> as a chemical feedstock starting with considering this molecule as a feedstock and not as a waste any longer.<sup>24</sup> For instance, very promising routes for the chemical conversion of CO<sub>2</sub> are the reverse water gas shift (RWGS) and dry reforming (DR)<sup>20</sup> processes to produce syngas and then fuel production thanks to the Fischer–Tropsch synthesis (FTS) catalytic process<sup>25,26</sup> or the methanol synthesis, which is another synthetic fuel. Methanol synthesis, FTS, and gas-to-liquid technologies are interesting enhancements that make carbon capture, utilization, and storage (CCUS) economically feasible.<sup>27</sup> Other chemical and industrial plants are also under investigation. For instance, CCUS would be applied to cement factories<sup>28</sup> and other nonconventional CO<sub>2</sub> emitters<sup>29–31</sup> (such as metallurgical processing, glass production furnaces, cement production, wastewater solids incineration, black liquor incineration at paper mills, municipal solid waste incineration) that require methanol as a conversion target. Hence, in the present work, we will mainly focus on the methanol sector whose impact on the reduction of CO<sub>2</sub> emissions and decarbonization has been already demonstrated.

In the methanol sector, despite continuous improvements in technologies and catalysts to reduce inefficiencies and energy dissipations, the kinetic models do not follow this trend.<sup>13</sup> As an instance of this; the kinetic path of methanol synthesis is not yet fully understood. The interactions among reactants and catalyst active sites are unclear, and the kinetic path (direct hydrogenation of CO and CO<sub>2</sub> to methanol) is not univocally defined.<sup>32–39</sup> According to the microkinetic approach, the methanol synthesis mechanisms may be separated into several elementary chemical steps.<sup>40–42</sup> In a recent publication, Lacerda de Oliveira Campos et al.<sup>43</sup> have proven the benefits of micro-kinetics in improving previous models by Slotboom<sup>44</sup> and Seidel.<sup>34</sup> However, to satisfy engineering purposes, the

methanol synthesis scheme is reduced to three reactions: (1) CO hydrogenation, (2) CO<sub>2</sub> hydrogenation, and (3) reverse water gas shift (RWGS)<sup>45–47</sup>



Several kinetic models have been published in the literature. These are listed in Table 1 and classified according to the carbon source that the kinetic scheme considers describing the methanol synthesis.

The original Graaf (or-GR)<sup>51</sup> and Vanden Bussche–Froment (VBF)<sup>55</sup> models are the ancestors of the kinetic models presented in Table 1, and the more recent additions may be considered as further development of these or just refit works where kinetic parameters are updated. Indeed, recently, several researchers published different refitted models based on or-GR and/or VBF kinetic structures. The resulting refitted kinetics are appreciable, and according to Slotboom<sup>44</sup> and Nestler,<sup>52</sup> respectively, their models are more accurate and reliable compared to the original ones thanks to in-house experiments and additional enhancements in microkinetic and mechanism modeling. However, these works lack outlier detection to prevent influential observations heavily impacting the regression of kinetic parameters. As emphasized in previous works by Buzzi-Ferraris and Manenti,<sup>57,58</sup> the gross errors and outliers are measurements (or more in general, data) that any possible model does not allow to interpret. Conversely, influential observations are data that the specific adopted model is not able to describe, but some others may. Hence, they heavily affect the regressed parameters and make the solver less effective and responsive in converging to the optimal solution. For instance, Slotboom and co-workers adopted the cross-validation method, but this does not

Table 2. Commercial Technologies for the Methanol Synthesis

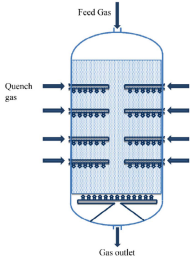
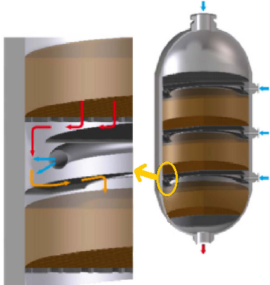
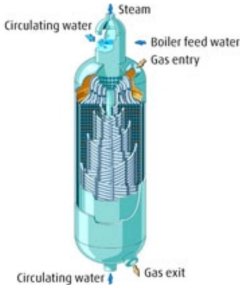
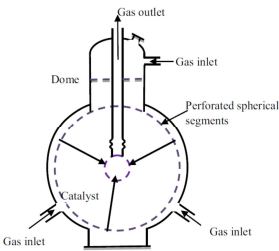
Company	Specifics	References
<p>Johnson Matthey</p> 	<ul style="list-style-type: none"> <li>• <math>50 &lt; P &lt; 100</math> bar</li> <li>• Ideal operating temperature 270°C</li> <li>• Quench reactor</li> <li>• Both radial and axial flow direction</li> <li>• Small scale applications (&lt; 2200 ton/day)</li> </ul>	<p>Wernicke et al. <sup>64</sup></p> <p>Bozzano and Manenti <sup>14</sup></p> <p>Dieterich et al. <sup>15</sup></p>
<p>ICI</p> 	<ul style="list-style-type: none"> <li>• Similar to Johnson Matthey</li> <li>• Improved quenching</li> <li>• Separated catalyst beds</li> <li>• Methanol production increased up to 20%</li> </ul>	<p>Graaf and Beenackers <sup>65</sup></p> <p>Bozzano and Manenti <sup>14</sup></p> <p>Dieterich et al. <sup>15</sup></p> <p>Westerterp et al. <sup>63</sup></p>
<p>Haldor Topsøe and Casale SA</p> 	<ul style="list-style-type: none"> <li>• Gas quench reactor (Haldor Topsøe) and boiling water (Casale SA)</li> <li>• Gas radial flow (catalytic part) and axial flow (quench)</li> <li>• Catalytic separated beds arranged plates</li> <li>• Reduced pressure drop</li> </ul>	<p>Wernicke et al. <sup>64</sup></p> <p>Tijm et al. <sup>62</sup></p> <p>Bozzano and Manenti <sup>14</sup></p> <p>Dieterich et al. <sup>15</sup></p>
<p>Kellogg Brown &amp; Root (KBR)</p> 	<ul style="list-style-type: none"> <li>• Series of adiabatic beds</li> <li>• Intermediate cooling</li> <li>• Spherical shape</li> </ul>	<p>Bozzano and Manenti <sup>14</sup></p> <p>Dieterich et al. <sup>15</sup></p> <p>Tijm et al. <sup>62</sup></p> <p>Westerterp et al. <sup>63</sup></p>

Table 2. continued

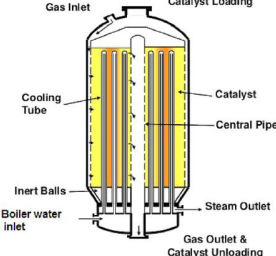
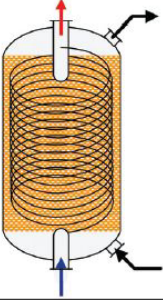
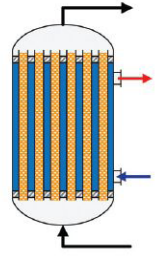
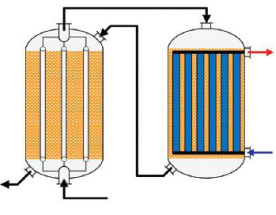
Company	Specifics	References
<p>Toyo Technology Company</p> 	<ul style="list-style-type: none"> <li>• Radial flow in concentric catalytic beds</li> <li>• Intermediate cooling with boiling water</li> <li>• Optimal temperature control</li> <li>• Low pressure drop</li> <li>• Easy scale-up</li> <li>• Small amount of catalyst (-30% regards conventional)</li> </ul>	<p>Bozzano and Manenti <sup>14</sup></p> <p>Dieterich et al. <sup>15</sup></p> <p>Hirotsu et al. <sup>74</sup></p> <p>Tijm et al. <sup>62</sup></p>
<p>Linde</p> 	<ul style="list-style-type: none"> <li>• Axial gas flow</li> <li>• Indirect cooling</li> <li>• Helical cooling tubes</li> <li>• Absence of radial temperature gradients</li> </ul>	<p>Lembeck <sup>75</sup></p> <p>Bozzano and Manenti <sup>14</sup></p> <p>Dieterich et al. <sup>15</sup></p>
<p>Lurgi (multitubular BWR)</p> 	<ul style="list-style-type: none"> <li>• Steam production (BWR)</li> <li>• Catalyst methanol yield (1.8 kg<sub>MeOH</sub> / L<sub>CZA</sub>)</li> <li>• Simple design and low manufacturing costs</li> </ul>	<p>Haid and Koss <sup>76</sup></p> <p>Wurzel <sup>77</sup></p> <p>Westerterp et al. <sup>63</sup></p>
<p>Lurgi (MegaMethanol)</p> 	<ul style="list-style-type: none"> <li>• Two reactors BWR and GCR</li> <li>• GCR works as gas preheater and methanol synthesis refinement (catalyst on shell-side)</li> <li>• Smaller BWR reactor</li> <li>• Low recycle ratio</li> </ul>	<p>Keramat et al. <sup>78</sup></p> <p>Wurzel <sup>77</sup></p> <p>Wernicke et al. <sup>64</sup></p> <p>Bozzano and Manenti <sup>14</sup></p> <p>Dieterich et al. <sup>15</sup></p> <p>Ott et al. <sup>67</sup></p>

Table 2. continued

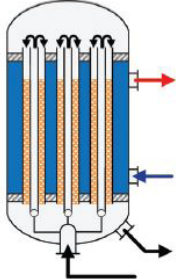
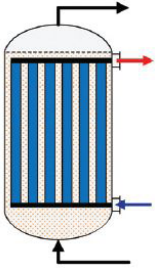
Company	Specifics	References
Mitsubishi Heavy Industries 	<ul style="list-style-type: none"> <li>• Double-walled pipes</li> <li>• Integrated BWR and CGR</li> <li>• Feed gas as coolant in the inner tube</li> <li>• Boiling water as coolant on the shell-side</li> <li>• Reaction in the annular section</li> </ul>	Wernicke et al. <sup>64</sup> Bozzano and Manenti <sup>14</sup> Tijm et al. <sup>62</sup>
AirProducts (LPMEOH) 	<ul style="list-style-type: none"> <li>• Slurry reactor</li> <li>• Pilot scale</li> <li>• Mild pressure (30-50 bar)</li> <li>• Low production volume (&lt; 2000 ton/day)</li> </ul>	Heydorn et al. <sup>69,79,80</sup> Dieterich et al. <sup>15</sup> Hansen and Højlund Nielsen <sup>66</sup> Tijm et al. <sup>62</sup>

Table 3. Additional Details on Commercial Technologies (Adapted from Dieterich<sup>15</sup>)

licensor	Lurgi	Linde	Toyo	Mitsubishi	Casale	Haldor Topsøe (HT)/ICI	AirLiquide MegaMethanol	AirProducts LPMEOH
reactor type	BWR	BWR	BWR	BWR/GCR	BWR	adiabatic	BWR/GCR	slurry
flow	axial	axial	axial/radial	axial	axial/radial	axial (ICI)/radial (HT)		
catalyst location	tube side	shell side	shell side	double pipe (annular)	shell side	fixed bed	shell side (GCR) and tube side (BWR)	shell side
heat exchanger	tubular	coil wound	bayonets	tubular	plates	intercool quenching	tubular	tubular
stages	1	1	1	1	1	2–5	2	1
<i>P</i> (bar)	50–100	50–150	80–100	55–100	65–80	50–100	60–75	30–50
<i>T</i> peak (°C)	270		280	270	280	290	270	215
<i>T</i> outlet (°C)	255		240	190	225		220	
pressure drop (bar)	3		0.3–0.5	2.4–7.5	1.1 (axial) 0.3 (radial)	2–3		3–5
recycling ratio <sup>a</sup>	3–4			2–3	3	3–5	2–2.7	1–5
conversion per pass <sup>b</sup> (%)	36		60	55–67			>80	20–50
MeOH outlet frac (mol %)	6–7		10	10–15	10–13.5	7	11	8–12
capacity (ton/day)	<2200	4000	5000		7000–10 000	10 000	5000–10 000	<2000
industrial plants	>55	8	6	9	9	>40	>15	1 pilot plant

<sup>a</sup>Recycling ratio is defined as recycled gas to fresh make-up on volume flow. <sup>b</sup>Conversion per pass defined as  $1 - \text{CO}_{X\text{-outlet}}/\text{CO}_{X\text{-inlet}}$  where  $\text{CO}_X$  is the sum of CO and  $\text{CO}_2$  molar flows.

guarantee that influential observations are completely removed and these have not affected the refitting procedure.<sup>57,59,60</sup> In the cross-validation method, the entire dataset is divided into an arbitrary number of subsets ( $N$ ). The regression procedure is repeated  $N$  times using  $N - 1$  subsets for the minimization procedure (training folder), while the last one is then used as a validation. In this procedure, each subset is used as a validation subset only one time and  $N - 1$  times in the regression

procedure. Among the  $N$  optimal solutions, the best one is selected according to statistical tests. In the case that the outliers or influential observation are uniformly distributed within the subsets, it is impossible to detect and remove them.<sup>60</sup> In the recent publication, Bisotti et al.<sup>13</sup> proposed an effective way to robustly refit the or-GR model obtaining a more flexible kinetic model for the prediction of methanol production over CZA catalyst in a wider operating range. We

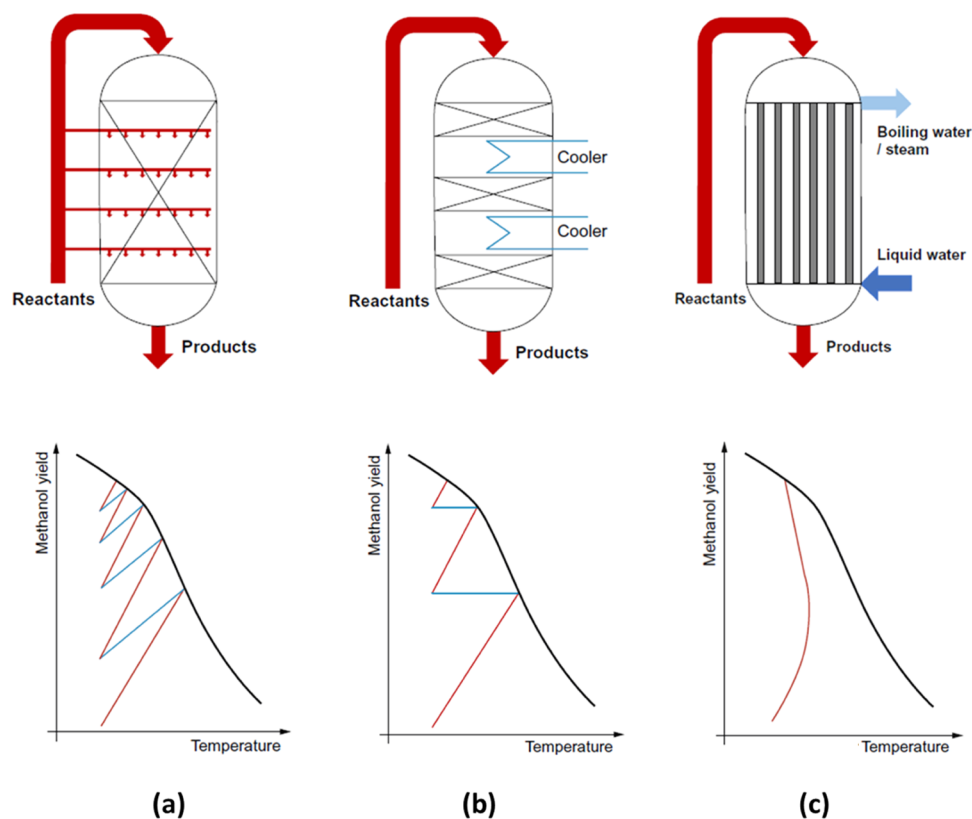


**Figure 1.** Temperature profile in most common commercial methanol technologies: (a) direct quenching (ICI), (b) indirect cooling (Haldor Topsoe, Casale SA, Toyo, and Mitsubishi), and (c) quasi-isothermal BWR (Lurgi). Picture adapted from Palma et al.<sup>71</sup>

refer to this refitted kinetic model as the ref-GR. The choice was to robustly update the Graaf's model since, first, it appears as the most complete kinetic model including the CO direct hydrogenation, and second, the VBF model seems to be already more accurate from a preliminary analysis. The proposed robust refit approach can be applied to any kinetics needing parameters update.<sup>13</sup>

The methanol rate of production and thermodynamic limitations are a direct consequence of the kinetics. In the literature, several papers analyzed different industrial technologies highlighting their advantages and the disadvantages of the competitors.<sup>14,15,61–65</sup> Many of these works show that the main target during reactor design is to guarantee the optimal temperature profile, thus minimizing as much as possible the reactor volume.<sup>66</sup> In the present work, we provide a brief resume of the main currently adopted technological solutions. The methanol reactor designs can be essentially classified according to the temperature profile and how the heat transfer is managed:<sup>45,61,67,68</sup> (1) adiabatic reactor with interstaged cooling provided by fresh syngas quenching or transfer line heat exchanger as in the ICI (now Johnson Matthey) technology, (2) quasi-isothermal reactor as in the boiling water reactor (BWR) as in Lurgi plants, or (3) double-reactor solution, where a gas-cooled reactor (GCR) is interconnected to the standard BWR (MegaMethanol, formerly a Lurgi solution, nowadays the AirLiquide technology). More recently, also slurry reactors are gaining attention due to their capacity to overcome shortcomings and limitations, which may arise using conventional methanol reactors such as mass transfer limitation and issues in heat removal, but the tests are still at the pilot plant scale.<sup>69,70</sup> Hence, this technological solution is not ready for the market owing to other drawbacks such as

downstream separation and pressure drop. Table 2 summarizes all of the current commercial solutions and the corresponding main features. It is noticeable that Lurgi (considering both the BWR and MegaMethanol) and ICI technologies represent more than 85% of the installed reactors worldwide as highlighted by Bozzano and Manenti.<sup>14</sup> Good references on the methanol reactor technologies are Bozzano and Manenti,<sup>14</sup> Dieterich et al.,<sup>15</sup> Tijm et al.,<sup>62</sup> Westerterp et al.,<sup>63</sup> and Palma et al.<sup>71</sup> Further works are Lange,<sup>61</sup> Cybulski,<sup>72</sup> and Klemes,<sup>73</sup> where advanced and innovative reactors are dealt with. Finally, Table 3 gathers additional technical details and further interesting pieces of information. In this table, we added also the slurry technology (denoted as AirProducts LPMEOH) since it is an appealing future enhancement in the methanol sector even though industrial plants have not been built yet.

From Table 3, it can be seen that the fixed-bed technology is nowadays dominating the market even though the slurry technology may be an alternative in the next future. The distinguishing elements among the several technologies are the production capacity, catalyst distribution/location, and heat management. The largest number of these technology exploits boiling water (BW) indirect cooling. This indirect cooling system guarantees an effective heat dissipation and, in principle, a quasi-isothermal internal temperature profile preventing hotspots if the tube bundle is properly designed.<sup>66,81,82</sup> The MegaMethanol takes advantage of gas indirect cooling in the pre-heater, leading to a smaller main reactor (BWR).<sup>15</sup> Moreover, the catalyst is deposited on the tube shell side enabling further methanol production. MegaMethanol is a consolidated technology for large-scale plants.<sup>78,79,83</sup> Mitsubishi and Toyo technologies exploit boiling water cooling combined with gas cooling thanks to a double-

Table 4. Analyzed Case Studies

technology	reference	adopted kinetic model	notes
Lurgi	Chen et al. <sup>87</sup>	VBF	196.0 ton/day methanol production (large-scale plant)
MegaMethanol	Keramat et al. <sup>78</sup> Rahmatmand et al. <sup>83</sup>	or-GR	both papers describe the same MegaMethanol plant in Shiraz; these papers deal with the same industrial plant and data; Keramat provides stream temperatures, while Rahmatmand includes the composition and reactors features
ICI	Al-Fadli et al. <sup>89</sup>	VBF	the authors present two different situations: real plant data (industrial case) and ICI company model for the reactor design (denoted as design); for both cases, we will compare the simulations results

pipe bundle. These solutions can effectively remove the reaction heating while also preheating the reactants (gas–gas heat exchanger) and generating water vapor (gas–transition phase liquid heat exchanger). In this configuration, the catalytic bed is inserted in the annular section of the double-pipe tube.<sup>62,64</sup> Finally, direct quenching is applied in the ICI design. During the direct quenching, the reactor undergoes a series of short catalytic fixed beds. The direct quenching design has two main advantages: (1) temperature reduction and (2) equilibrium shifting. Both effects positively impact the thermodynamic equilibrium involved in the methanol synthesis.<sup>14,71</sup> Considering the operations, radial reactors guarantee low pressure drops and more compact units. This also leads to an easier reactor and process scale-up as highlighted in different works.<sup>15,45,46,74–76</sup> It is not clear which is the best technology; however, the reactor technology selection is essentially driven by plant size. For small-scale plants (<2200 ton/day), the Lurgi single-stage technology (BWR) is the most economically profitable solution, whereas for large-scale plants (>7000 ton/day), the MegaMethanol and ICI solutions compete for best results. In addition, the MegaMethanol technology enables us to improve the overall methanol production due to a double-integrated reactor system, but as mentioned before, it is appealing only for large and well-integrated production sites. On the other hand, the Wurzel report clearly depicts that the Lurgi technology is not an optimized solution.<sup>77,84</sup> For instance, considering the Lurgi technology as a benchmark, the MegaMethanol plant requires at least +30% in CapEx, but it enables us to reduce the overall OpEx up to –5% thanks to energy integrations. Further, the final result is a doubled methanol production with lower methane consumption (i.e., lower CO<sub>2</sub> and greenhouse gases footprint) and a lower methanol production cost (reduced by –20%). Also, the heat removal system has an impact on the technology selection since it influences the reaction rates and the mixture of final products. Figure 1 depicts the temperature profiles in the industrial technologies adopted in the methanol production. In this case, the analysis is limited to fixed-bed technologies. The ideal temperature profile would lead to an optimal process configuration such that the production is always the maximum and side reactions such as methanation that may arise thermal energy dissipation concerns<sup>45,46</sup> are avoided. The quasi-isothermal reactor design is very close to the optimal solution; however, adiabatic bed reactors are common in the industry since the lower temperature control and higher thermodynamic limitations are usually offset by the faster kinetics at a higher temperature. Methanol production is thermodynamically favored at low temperatures, but kinetics always favor higher temperatures. The slurry reactor design is the only alternative to the fixed-bed reactor.<sup>66,69,80</sup> In this technology, fine solid catalyst particles are suspended into an inert oil. The inlet gas and the recycled liquid phase guarantee the agitation and fluidization of

powders. The slurry phase process has the advantage of the absence of diffusion limitations and an optimal temperature control as it is typical in continuous stirred-tank reactor (CSTR) reactors. In fact, the slurry bed fluidization theoretically leads to uniform temperature and optimal heat energy distribution and discharge. This is possible thanks to the liquid (slurry)–liquid (boiling water) heat exchanger, which exhibits a higher heat transfer coefficient with respect to the conventional fixed-bed heat exchangers.<sup>69,80</sup> On the other hand, it incurs higher investment costs due to larger volume since the slurry solution maximum catalyst loading is 50% w/w. In addition, it presents some difficulties in the product recovery.<sup>66</sup> Indeed, as Beenackers highlights,<sup>70</sup> the two main disadvantages related to the slurry technology are the downstream separation and the pressure management. Indeed, the catalyst powders are dispersed in a slurry viscous solution where the produced methanol is entrapped and kept into the liquid phase. Thus, the downstream processes are costly owing to the difficulties in liquid/solid separation. Moreover, the gas phase undergoes a large pressure drop, meaning that the recompression expenses are not negligible.

After this brief introduction on the methanol synthesis kinetics and current reactor technologies, the present work aims at comparing the methanol synthesis predictions over the CZA catalyst for three kinetics (limited to or-GR, VBF, and ref-GR models) for different reactor configurations such as Lurgi reactor (BWR), MegaMethanol (combined BWR and CGR reactors system), and ICI converter (adiabatic gas quenched configuration). The analysis has been limited to these three kinetics since as mentioned above, or-GR and VBF kinetics are considered an industrial benchmark for methanol synthesis modeling<sup>73,78,85,86</sup> and we wish to prove that ref-GR is a reliable kinetic model suitable for reactor design and process simulation. In a similar manner, only the Lurgi (both single-staged BWR and MegaMethanol now licensed by AirLiquide) and ICI (now Johnson Matthey) technologies have been considered in the light of their dominant market share (87% until 2016).<sup>14,15</sup> The reactor designs in this work have been fully performed within the industrial process simulator Aspen HYSYS. Other tools, such as programming languages and/or plug in external model, are not necessary unless the user wishes to optimize the reactor configuration, reactor internal temperature profile, minimize the catalyst amount, or accomplish other tasks other than process simulation. Conversely to previous similar works where kinetics models are analyzed in parallel to show the main discrepancies and different predictions both in the methanol formation and final product mixture composition,<sup>82</sup> here, the obtained results are compared with industrial data published in the literature<sup>78,83,87–89</sup> including technologies different from BWR. The usage of industrial data for validation is the topic of this paper since ref-GR with lab-scale reactor experimental datasets has already been validated in a previous study.<sup>13</sup> Here,

Table 5. Binary Interaction Coefficient for the SRK Model in the HYSYS Thermodynamic Group

	CO	CO <sub>2</sub>	H <sub>2</sub>	H <sub>2</sub> O	CH <sub>4</sub>	N <sub>2</sub>	O <sub>2</sub>	CH <sub>3</sub> OH
CO		0.1164	$-7.00 \times 10^{-4}$	-0.5594	$2.04 \times 10^{-2}$	$1.30 \times 10^{-2}$	0	0
CO <sub>2</sub>	0.1164		0.1164	-0.12155	$9.56 \times 10^{-2}$	$-1.71 \times 10^{-2}$	$9.75 \times 10^{-2}$	$1.70 \times 10^{-2}$
H <sub>2</sub>	$-7.00 \times 10^{-4}$	0.1164		-0.7544	$1.00 \times 10^{-4}$	$-1.00 \times 10^{-3}$	0	0
H <sub>2</sub> O	-0.5594	-0.12155	-0.7544		0.5	-0.69648	0	$-9.00 \times 10^{-2}$
CH <sub>4</sub>	$2.04 \times 10^{-2}$	$9.56 \times 10^{-2}$	$1.00 \times 10^{-4}$	0.5		$3.12 \times 10^{-2}$	0	$-3.50 \times 10^{-2}$
N <sub>2</sub>	$1.30 \times 10^{-2}$	$-1.71 \times 10^{-2}$	$-1.00 \times 10^{-3}$	-0.69648	$3.12 \times 10^{-2}$		$-1.40 \times 10^{-2}$	-0.2141
O <sub>2</sub>	0	$9.75 \times 10^{-2}$	0	0	0	$-1.40 \times 10^{-2}$		0
CH <sub>3</sub> OH	0	$1.70 \times 10^{-2}$	0	$-9.00 \times 10^{-2}$	$-3.50 \times 10^{-2}$	-0.2141	0	

Table 6. Kinetics of the Original Structure as Proposed in Reference Works

kinetic model	rates (mol/(kg <sub>cat</sub> ·s))
Graaf (or-GR) and refitted Graaf (ref-GR)	$r_{\text{CO}_2/\text{MeOH}} = \frac{k_1 K_{\text{CO}_2} \left( f_{\text{CO}_2} f_{\text{H}_2}^{3/2} - \frac{f_{\text{MeOH}} f_{\text{H}_2\text{O}}}{f_{\text{H}_2}^{3/2} K_{\text{eqCO}_2}} \right)}{\left( 1 + K_{\text{CO}} f_{\text{CO}} + K_{\text{CO}_2} f_{\text{CO}_2} \right) \left( f_{\text{H}_2}^{1/2} + \left( K_{\text{H}_2\text{O}}/K_{\text{H}_2}^{1/2} \right) f_{\text{H}_2\text{O}} \right)}$ $r_{\text{RWGS}} = \frac{k_2 K_{\text{CO}_2} \left( f_{\text{CO}_2} f_{\text{H}_2} - \frac{f_{\text{H}_2\text{O}} f_{\text{CO}}}{K_{\text{eqRWGS}}} \right)}{\left( 1 + K_{\text{CO}} f_{\text{CO}} + K_{\text{CO}_2} f_{\text{CO}_2} \right) \left( f_{\text{H}_2}^{1/2} + \left( K_{\text{H}_2\text{O}}/K_{\text{H}_2}^{1/2} \right) f_{\text{H}_2\text{O}} \right)}$ $r_{\text{CO}/\text{MeOH}} = \frac{k_3 K_{\text{CO}} \left( f_{\text{CO}} f_{\text{H}_2}^{3/2} - \frac{f_{\text{MeOH}}}{f_{\text{H}_2}^{1/2} K_{\text{eqCO}}} \right)}{\left( 1 + K_{\text{CO}} f_{\text{CO}} + K_{\text{CO}_2} f_{\text{CO}_2} \right) \left( f_{\text{H}_2}^{1/2} + \left( K_{\text{H}_2\text{O}}/K_{\text{H}_2}^{1/2} \right) f_{\text{H}_2\text{O}} \right)}$
Vanden Bussche–Froment (VBF)	$r_{\text{CO}_2/\text{MeOH}} = \frac{k_1 p_{\text{CO}_2} p_{\text{H}_2} \left( 1 - \frac{p_{\text{MeOH}} p_{\text{H}_2\text{O}}}{p_{\text{H}_2}^3 p_{\text{CO}_2} K_{\text{eqCO}_2}} \right)}{\left( 1 + K_1 \frac{p_{\text{H}_2\text{O}}}{p_{\text{H}_2}} + \sqrt{K_2 p_{\text{H}_2}} + K_3 p_{\text{H}_2\text{O}} \right)^3}$ $r_{\text{CO}_2/\text{MeOH}} = \frac{k_2 p_{\text{CO}_2} \left( 1 - \frac{p_{\text{CO}} p_{\text{H}_2\text{O}}}{p_{\text{H}_2} p_{\text{CO}_2} K_{\text{eqRWGS}}} \right)}{\left( 1 + K_1 \frac{p_{\text{H}_2\text{O}}}{p_{\text{H}_2}} + \sqrt{K_2 p_{\text{H}_2}} + K_3 p_{\text{H}_2\text{O}} \right)}$

Table 7. Original Kinetic and Thermodynamic Parameters for the Considered Kinetics<sup>a,b</sup>

parameters	or-GR	ref-GR	VBF
kinetic coefficients	$k_1 = 1.09 \times 10^5 e^{-(87\,500/RT)}$ $k_2 = 9.64 \times 10^{11} e^{-(152\,900/RT)}$ $k_3 = 4.89 \times 10^7 e^{-(11\,300/RT)}$	$k_1 = 9.205 \times 10^1 e^{-(45\,889/RT)}$ $k_2 = 4.241 \times 10^{13} e^{-(149\,856/RT)}$ $k_3 = 2.240 \times 10^7 e^{-(106\,729/RT)}$	$k_1 = 1.07 \times 10^1 e^{-(36\,696/RT)}$ $k_2 = 1.22 \times 10^{10} e^{-(94\,765/RT)}$
adsorption constants	$K_{\text{CO}_2} = 7.05 \times 10^{-7} e^{61\,700/RT}$ $K_{\text{CO}} = 2.16 \times 10^{-5} e^{46\,800/RT}$ $K_{\text{H}_2\text{O}}/K_{\text{H}_2}^{1/2} = 6.37 \times 10^{-9} e^{84\,000/RT}$	$K_{\text{CO}_2} = 8.206 \times 10^{-9} e^{76\,594/RT}$ $K_{\text{CO}} = 1.540 \times 10^{-3} e^{14\,936/RT}$ $K_{\text{H}_2\text{O}}/K_{\text{H}_2}^{1/2} = 3.818 \times 10^{-9} e^{97\,350/RT}$	$K_1 = 3.45 \times 10^3$ $\sqrt{K_2} = 4.99 \times 10^{-1} e^{17\,197/RT}$ $K_3 = 6.62 \times 10^{-11} e^{124\,119/RT}$
equilibrium constants	$\log_{10}(K_{\text{eq,CO}_2}) = \frac{3066}{T} - 10.592$ $\log_{10}(K_{\text{eq,RWGS}}) = -\frac{2073}{T} + 2.029$ $\log_{10}(K_{\text{eq,CO}}) = \frac{5139}{T} - 12.621$		$\log_{10}(K_{\text{eq,CO}_2}) = \frac{3066}{T} - 10.592$ $\log_{10}(K_{\text{eq,RWGS}}) = -\frac{2073}{T} + 2.029$

<sup>a</sup>Activation energy are expressed in J/mol,  $P$  in bar, and  $T$  in K. <sup>b</sup>Fugacity estimated using the SRK equation of state.

we wish to demonstrate the effectiveness of its implementation and application also for industrial purposes. The analysis will show a good agreement between the industrial data and the ref-GR predictions, confirming the considerations and predictive accuracy as in the previous publication.<sup>13</sup> These results further attest that ref-GR is a suitable tool to design methanol reactors outperforming the original Graaf independently from the adopted technology.

## METHODS

**Industrial Data.** Considering the main target of the present work, we focused our efforts on searching reliable industrial data published in the literature. The data of selected papers have been used to validate the refitted Graaf (ref-GR) and compare its performance with respect to the original model (or-GR)<sup>51</sup> and the Vanden Bussche–Froment (VBF)<sup>55</sup> one. As already discussed, the or-GR and VBF kinetics are the most consolidated and adopted models in industrial practice.<sup>73,78,85,86</sup> Table 4 lists the proposed industrial case studies,



Table 8. Reformulated Reaction Rates (Compliant with the Aspen HYSYS PFR Reactor)

kinetic	reaction	rates (mol/(kg <sub>cat</sub> ·s))
or-GR ref-GR	CO <sub>2</sub> hydrogenation (1)	$r_{\text{CO}_2 \rightarrow \text{MeOH}} = \frac{k_1 K_{\text{CO}_2} f_{\text{CO}_2}^{1.5} - \frac{k_1 K_{\text{CO}_2}}{K_{\text{eqCO}_2}} f_{\text{MeOH}} f_{\text{H}_2} f_{\text{H}_2}^{-1.5}}{1 + K_{\text{CO}} f_{\text{CO}} + K_{\text{CO}_2} f_{\text{CO}_2}^{0.5} + K_{\text{CO}_2} \frac{K_{\text{H}_2\text{O}}}{K_{\text{H}_2}^{0.5}} f_{\text{CO}_2} f_{\text{H}_2\text{O}}}$
	RWGS (2)	$r_{\text{RWGS}} = \frac{k_2 K_{\text{CO}_2} f_{\text{CO}_2} f_{\text{H}_2} - \frac{k_2 K_{\text{CO}_2}}{K_{\text{eqRWGS}}} f_{\text{H}_2} f_{\text{CO}}}{1 + K_{\text{CO}} f_{\text{CO}} + K_{\text{CO}_2} f_{\text{CO}_2}^{0.5} + K_{\text{CO}_2} \frac{K_{\text{H}_2\text{O}}}{K_{\text{H}_2}^{0.5}} f_{\text{CO}_2} f_{\text{H}_2\text{O}}}$
	CO hydrogenation (3)	$r_{\text{CO} \rightarrow \text{MeOH}} = \frac{k_3 K_{\text{CO}} f_{\text{CO}_2}^{1.5} - \frac{k_3 K_{\text{CO}}}{K_{\text{eqCO}}} f_{\text{MeOH}} f_{\text{H}_2}^{-0.5}}{1 + K_{\text{CO}} f_{\text{CO}} + K_{\text{CO}_2} f_{\text{CO}_2}^{0.5} + K_{\text{CO}_2} \frac{K_{\text{H}_2\text{O}}}{K_{\text{H}_2}^{0.5}} f_{\text{CO}_2} f_{\text{H}_2\text{O}}}$
VBF	CO <sub>2</sub> hydrogenation (1)	$r_{\text{CO}_2 \rightarrow \text{MeOH}} = \frac{k_1^{\text{P}} p_{\text{CO}_2} p_{\text{H}_2} - \frac{k_1}{K_{\text{eqCO}_2}} p_{\text{MeOH}} p_{\text{H}_2} p_{\text{H}_2}^{-2}}{\left(1 + K_1 \frac{p_{\text{H}_2\text{O}}}{p_{\text{H}_2}} + \sqrt{K_2} p_{\text{H}_2}^{0.5} + K_3 p_{\text{H}_2\text{O}}\right)^3}$
	RWGS (2)	$r_{\text{RWGS}} = \frac{k_2^{\text{P}} p_{\text{CO}_2} - \frac{k_2}{K_{\text{eqRWGS}}} p_{\text{CO}} p_{\text{H}_2} p_{\text{H}_2}^{-1}}{1 + K_1 \frac{p_{\text{H}_2\text{O}}}{p_{\text{H}_2}} + \sqrt{K_2} p_{\text{H}_2}^{0.5} + K_3 p_{\text{H}_2\text{O}}}$

Table 9. Kinetic Parameters of the Reformulated Model/Activation Energy (J/mol)

reaction	kinetic parameters	or-GR			ref-GR			BVF		
		A	β	E <sub>act</sub>	A	β	E <sub>act</sub>	A	β	E <sub>act</sub>
CO <sub>2</sub> hydrogenation	k <sub>dir</sub>	7.68 × 10 <sup>-2</sup>	0	2.58 × 10 <sup>4</sup>	7.55 × 10 <sup>-7</sup>	0	-3.07 × 10 <sup>5</sup>	1.07	0	-3.67 × 10 <sup>4</sup>
	k <sub>rev</sub>	3.01 × 10 <sup>9</sup>	0	8.45 × 10 <sup>4</sup>	2.95 × 10 <sup>4</sup>	0	2.80 × 10 <sup>4</sup>	4.18 × 10 <sup>10</sup>	0	2.20 × 10 <sup>4</sup>
RWGS	k <sub>dir</sub>	6.80 × 10 <sup>5</sup>	0	9.12 × 10 <sup>4</sup>	3.48 × 10 <sup>5</sup>	0	7.33 × 10 <sup>4</sup>	1.22 × 10 <sup>10</sup>	0	9.48 × 10 <sup>4</sup>
	k <sub>rev</sub>	6.36 × 10 <sup>3</sup>	0	5.15 × 10 <sup>4</sup>	3.26 × 10 <sup>3</sup>	0	3.36 × 10 <sup>4</sup>	1.14 × 10 <sup>8</sup>	0	5.51 × 10 <sup>4</sup>
CO hydrogenation	k <sub>dir</sub>	1.06 × 10 <sup>3</sup>	0	6.62 × 10 <sup>4</sup>	3.45 × 10 <sup>4</sup>	0	9.18 × 10 <sup>4</sup>			
	k <sub>rev</sub>	4.41 × 10 <sup>15</sup>	0	1.65 × 10 <sup>5</sup>	1.44 × 10 <sup>17</sup>	0	1.90 × 10 <sup>5</sup>			

Table 10. Parameters for Adsorption Constants (Adsorption Energy in J/mol)<sup>a</sup>

adsorption constants	or-GR		ref-GR		adsorption constants	BVF	
	B	E <sub>ads</sub>	B	E <sub>ads</sub>		B	E <sub>ads</sub>
K <sub>CO</sub>	2.16 × 10 <sup>-5</sup>	-4.68 × 10 <sup>4</sup>	1.54 × 10 <sup>-3</sup>	-1.49 × 10 <sup>-4</sup>	K <sub>1</sub>	3.45 × 10 <sup>3</sup>	
K <sub>CO<sub>2</sub></sub>	7.05 × 10 <sup>-7</sup>	-6.17 × 10 <sup>4</sup>	8.21 × 10 <sup>-9</sup>	-7.66 × 10 <sup>4</sup>	√K <sub>2</sub>	4.99 × 10 <sup>-1</sup>	-1.72 × 10 <sup>4</sup>
K <sub>ADS</sub> <sup>a</sup>	6.37 × 10 <sup>-9</sup>	-8.40 × 10 <sup>4</sup>	3.82 × 10 <sup>-9</sup>	-9.74 × 10 <sup>4</sup>	K <sub>3</sub>	6.62 × 10 <sup>-11</sup>	-1.24 × 10 <sup>5</sup>

$$^a K_{\text{ADS}} = K_{\text{CO}_2} \cdot \frac{K_{\text{H}_2\text{O}}}{K_{\text{H}_2}^{0.5}}$$

which are clustered according to the reactor technology. We would like to remark that the current analysis is mainly focused on BWR (Lurgi), MegaMethanol (AirLiquide), and adiabatic fixed-bed configuration (Johnson Matthey, formerly ICI) since these are the most relevant and widespread reactor technologies in the methanol sector.

**Implementation.** The analyzed case studies have been implemented in Aspen HYSYS V11. The details for the implementation of each case study (such as operating conditions, feed flow and composition, reactor design) are provided in the corresponding paragraph in the Results and Discussion section. The general simulation setup is described here. The Soave–Redlick–Kwong (SRK) equation of state (EoS) is adopted to characterize the thermodynamic properties of the mixtures (wet syngas and methanol) as suggested in previous studies<sup>44,52,90</sup> and is compliant with the refit procedure in Bisotti et al.<sup>13</sup> We adopted the SRK thermodynamic model from the HYSYS list (not the Aspen Properties one). The component list includes CO, CO<sub>2</sub>, H<sub>2</sub>, H<sub>2</sub>O (steam), methane, nitrogen, oxygen, and methanol. Furtherly, we left the default setting and the component

properties from the HYSYS list. Hence, the binary interaction coefficients have been kept (see Table 5).

Concerning the kinetic models, the kinetic parameters are taken from the corresponding references: or-GR,<sup>51</sup> ref-GR,<sup>13</sup> and VBF.<sup>55</sup> Table 6 reports the original expression for the considered kinetics, while Table 7 reports the corresponding values for the kinetic parameters, adsorption, and equilibrium constants.

Since the Aspen HYSYS suite requires a specific parametric formula for the reaction rates, the kinetic models should be reformulated to be compliant with the software requirements. This general form follows the structure of Langmuir–Hinshelwood–Hougen–Watson (LHHW)-type kinetics. The general rate in Aspen HYSYS is

$$r = \frac{k_{\text{dir}} \cdot f_{\text{dir}}(P_i) - k_{\text{rev}} \cdot f_{\text{rev}}(P_i)}{\left[1 + \sum_{i=1}^N K_i \cdot f_i(P_i)\right]^n} \quad (1)$$

where  $k_{\text{dir}}$  and  $k_{\text{rev}}$  are the kinetic constants of the direct and reverse reactions, respectively, and  $K_i$  is the adsorption parameters appearing in the denominator. The terms at the numerator  $f_{\text{dir}}(P_i)$  and  $f_{\text{rev}}(P_i)$  are functions of the species

Table 11. Parameters in Equilibrium Constants (Adsorption Energy in J/mol)

equilibrium constants	or-GR		ref-GR		VBF	
	$B$	$E_{\text{ads}}$	$B$	$E_{\text{ads}}$	$B$	$E_{\text{ads}}$
$K_{\text{eq,CO}_2}$	$2.56 \times 10^{-11}$	$-5.87 \times 10^4$	$2.56 \times 10^{-11}$	$-5.87 \times 10^4$	$2.56 \times 10^{-11}$	$-5.87 \times 10^4$
$K_{\text{eq,RWGS}}$	$1.07 \times 10^2$	$3.97 \times 10^4$	$1.07 \times 10^2$	$3.97 \times 10^4$	$1.07 \times 10^2$	$3.97 \times 10^4$
$K_{\text{eq,CO}}$	$2.39 \times 10^{-13}$	$-9.84 \times 10^4$	$2.39 \times 10^{-13}$	$-9.84 \times 10^4$		

fugacity. The kinetic constants and the adsorption parameters are defined according to the conventional Arrhenius law

$$k_j = A_j \cdot T^{\beta_j} \exp\left(-\frac{E_j}{RT}\right) \quad (2)$$

$$K_i = B_i \exp\left(-\frac{E_i}{RT}\right) \quad (3)$$

Hence, the or-GR, ref-GR, and VBF kinetics are rewritten accordingly (VBF is already predisposed for this refinement). We provide a reformulated form of the three analyzed kinetics (Table 8) and the corresponding value for the kinetic parameters (Tables 9–11). These values are the ones adopted throughout all of the case studies. We would remark that the proposed kinetics is based on the mass of the catalyst. Aspen HYSYS works with kinetic rates expressed per unit of reactor volume; hence, it is necessary to know the catalyst density and the void fraction within the packed bed (also these pieces of information are given for all of the analyzed cases). The pressure drop along the tube bundle is estimated using the Ergun method implemented in Aspen HYSYS V11.

Finally, Rahimpour and collaborators suggest adopting the heterogeneous model to characterize the reactive system since for temperatures larger than 260 °C (close to temperature peak in BWR), the catalyst may suffer mass diffusion limitations. However, neither the results they provided<sup>83,90,91</sup> nor other works<sup>81,82,92–94</sup> detected a significant impact of the mass transfer limitations. Thus, it is reasonable to directly implement the kinetic models into the plug flow reactor (PFR) in Aspen HYSYS V11 neglecting the catalyst efficiency (i.e., pseudo-homogeneous model without temperature and concentration gradients within the catalyst particle) and the radial gradients as well. The last assumption is a common practice adopted also in the already cited works. As mentioned in the Introduction—A Brief Introduction on the Methanol Synthesis Kinetics and Reactor Technologies section, the present work aims at comparing the predictions of the kinetic models for the most widespread methanol synthesis technologies using commercial simulation software (Aspen HYSYS) and taking advantage of real industrial plant data. For this reason, the detailed mathematical modeling and the related implementation through programming languages such as Matlab or similar ones are considered out of the scope. There is space for a final warning. As stated by George Box, “all models are wrong, but some are useful”, we would remark that this point should be kept in mind when dealing with modeling and model validation. The present work started with the purpose of correcting the issue for the discussed kinetic models. From the way we see it, the original kinetic models we refitted incorporated themselves the “salient details” of the technologies of their time because that is what a statistical model does. Over time, the technologies became outdated and were changed for more modern solutions, but the kinetic models were left. In our vision, this created a discrepancy between the

“salient details” that are included in the kinetic models and the ones that are present in modern technologies. In addition to this, we would say that neither sophisticated model is able to catch all of the aspects involved in a model such as back mixing, reactants mixing, stagnant part, channeling, and so forth. This means that we need to accept simplifications, simplified models, and modeling whenever reasonable. In the case that the outputs are close to the expected results, it means that the assumptions are correct to accurately describe the average properties of the system. Finally, it is important to remark that the regression procedure tends to reduce the error and often to fragment and spread it over all of the experimental observations to bridge the gap for the overall points included in the dataset. This implies that also the residual error will be distributed in each node of the discretization for the reactor. The perfect model does not exist. The possibility to increase model complexity is really appealing, but focus must be also be given to the computational time and the maximum level of accuracy that such models can reach.

## RESULTS AND DISCUSSION

**Lurgi Technology (BWR).** The Lurgi technology consists of a tube bundle submerged in a boiling water (BW) bath. The boiling water (Boiling Water) continuously evaporates, generating saturated steam (Steam out) while reaction heat (Heat) release occurs within the tubes filled with catalyst powders (LURGI). The syngas mixture (Syngas Feed) generally passes through the tubes from top to bottom. The final mixture (Product out) is sent to the downstream units for purification. It is one of the easiest reactor solutions since rotating mechanical parts and gas distributor (such as in the ICI quenching) are missing. The BWR can be simulated as a conventional PFR where the heat transfer and all geometrical features are defined. The released heat is then passed to a heater heat exchanger where steam is generated. The Lurgi basic flowsheet is depicted in Figure 2. We propose hereafter several different industrial applications.

Chen et al.<sup>87</sup> recently published a work dealing with the modeling of an industrial Lurgi reactor proving also plant data. The reactor specifications and the input data are gathered in

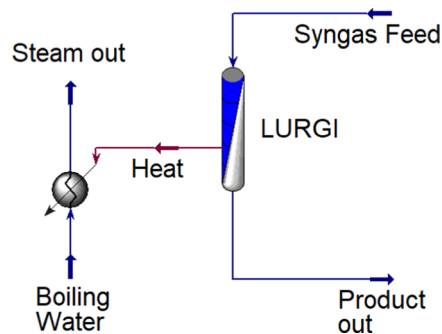


Figure 2. Lurgi reactor simulation flowsheet.

Tables 12 and 13, respectively. Conversely to the cited work, we neglected the production of higher alcohols and methyl

**Table 12. Reactor and Catalyst Specifications**

reactor tube diameter (m)	0.04
reactor length (m)	7
number of tubes	1620
catalyst diameter (mm)	5.4
catalyst particle density (kg/m <sup>3</sup> )	1190
void fraction of the bed	0.285
heat transfer coefficient (W/(m <sup>2</sup> ·K))	118.44

**Table 13. Feed (Syngas Feed) and Coolant (Boiling Water) Specifications**

	syngas feed	boiling water
temperature (°C)	225	220
pressure (bar)	69.7	29
molar flow rate (kmol/h)	6264.8	
mass flow rate (kg/h)	57 269	13 800
vapor fraction	1	0
component flow rate (kg/h)		
CO	10 727.9	
CO <sub>2</sub>	23 684.2	
H <sub>2</sub>	9586.5	
H <sub>2</sub> O	108.8	13 800
methanol	756.7	
CH <sub>4</sub>	4333.1	
N <sub>2</sub>	8072.0	

formate since their formation rates are not included within the analyzed kinetic models. This approximation is deemed acceptable considering that these side products constitute 0.06% (on mass base) of the final composition according to the plant data. For this reason, these are not reported in the input data table and not considered in the total flow mass rate. Moreover, we consider the steam vapor fraction and steam temperature as additional variables for the problem since the simulator enables us to estimate these values once the transferred heat is determined. Finally, the provided heat transfer coefficient is in line with typical ranges as in other works.<sup>95,96</sup>

The results are gathered in Table 14, and the main parameter profiles within the reactor are depicted in Figures 3 and 8. In the results table, the nitrogen and methane mass

flows are not reported since these compounds are inert in the methanol synthesis reactor, thus constant along the reactor length. The results show good agreement between the industrial data and the ref-GR kinetic. With the only exception of the CO content, the ref-GR properly describes the composition in the Lurgi technology. For instance, just considering the reactive section, the average error is below 3.5% and the CO content prediction deviates by 8%. The VBF model exhibits a similar accuracy even though it presents larger deviations especially in the predictions of CO, steam, and methanol contents (relative errors larger than 7%). Conversely, or-GR is completely inaccurate and provides unreliable outputs as also shown in Figure 3. Using the or-GR model, the Aspen solver for the differential balance in PFR predicts a closely isothermal reactor, leading to an underestimation of the methanol productivity in the Lurgi reactor. The present case study confirms and supports the conclusion provided in a previous study,<sup>13</sup> where the inaccuracy of the or-GR model was highlighted as it underestimates the methanol content in the product mixture. Moreover, it is proven that the refit procedure benefits the kinetic model, making it more robust and reliable. Finally, it is remarkable that there exists a discrepancy between the produced steam and the industrial data. This is explainable considering that the estimated saturation temperature does not coincide with the measured one. This may mean that the SRK EoS does not correctly determine the water boiling point, or the steam is superheated steam. The second option would not be confirmed since Chen and co-workers report the vapor fraction in the produced steam. However, in the reference, there are no explanations for how such a measurement was managed in the industrial plant.

**MegaMethanol (AirLiquide).** The MegaMethanol technology (Figure 4) is an enhancement of the BWR or single-staged Lurgi one. The gas is preheated in the gas-cooled reactor (GCR) on the left-hand side in Figure 4, while the product mixture exiting the conventional BWR undergoes a further refinement thanks to the increase of methanol productivity. In the GCR, the reaction occurs under milder conditions since the gas cooling is not as effective as where a transition phase liquid acts as a coolant.

Figure 5 depicts the implementation of the MegaMethanol technology in Aspen HYSYS. The cold feed (COLD SYNGAS) is preheated exploiting the duty released ( $Q_{GCR}$ ) in the gas-cooled reactor (GCR), where the intermediate product mixture (stream 7) is further refined to increase the

**Table 14. Results and Comparison of Lurgi Reactor Simulation as in Chen et al.<sup>87</sup>**

	industrial	ref-GR		VBF		or-GR	
		value	rel error (%)	value	rel error (%)	value	rel err (%)
product out							
temperature (°C)	255.0	258.5	−1.373	255.3	−0.118	232.0	9.020
pressure (bar)	66.7	66.71	−0.015	66.73	−0.045	66.73	−0.045
component flow (kg/h)							
CO	4921	5321.18	−8.132	5682.92	−15.483	9886.05	−100.895
CO <sub>2</sub>	18 316.4	18 127.56	1.031	18 749.84	−2.366	21 235.30	−15.936
H <sub>2</sub>	8013.7	8044.62	−0.386	8182.18	−2.102	9128.79	−13.915
H <sub>2</sub> O	2309.3	2383.42	−3.210	2128.74	7.819	1111.24	51.880
MeOH	11 283.1	10 987.13	2.623	10 120.5	10.304	3502.68	68.956
steam out							
vapor fraction	0.805	0.7747	3.764	0.7128	11.453	0.1652	79.478
temperature (°C)	231.2	233.5	−0.995	233.5	−0.995	233.5	−0.995

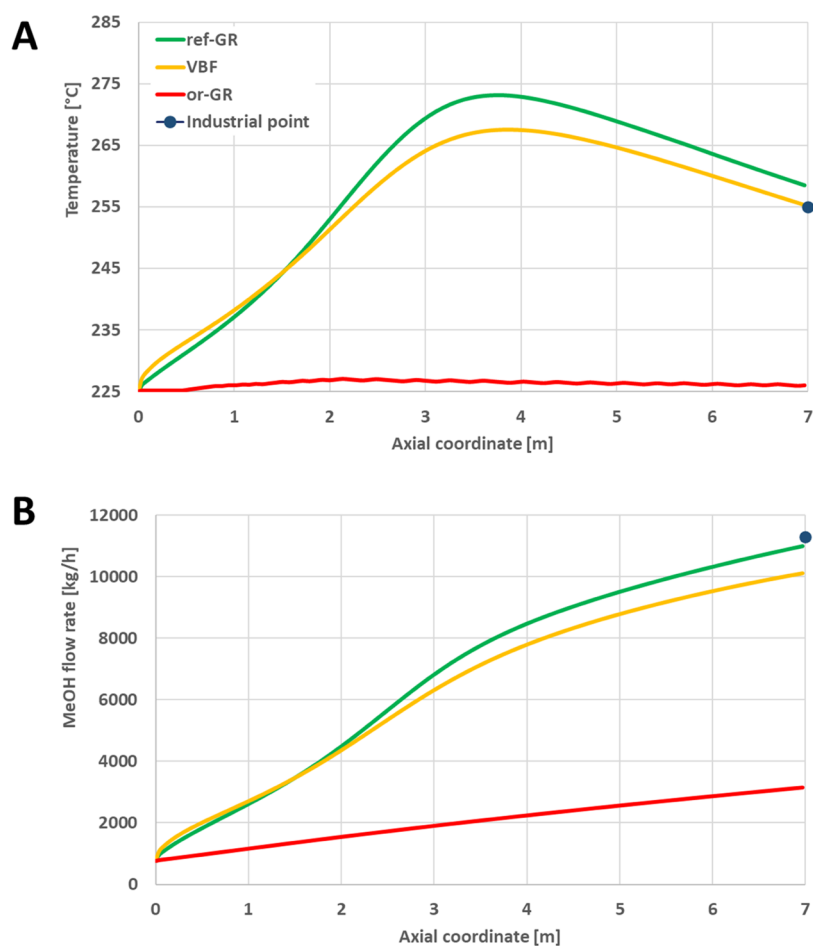


**Figure 3.** Temperature profile (A) and methanol mass flow rate (B) in the Lurgi reactor in Aspen HYSYS: ref-GR (green), VBF (yellow), and or-GR (red). The dot indicates the industrial data provided in Chen et al.<sup>87</sup>

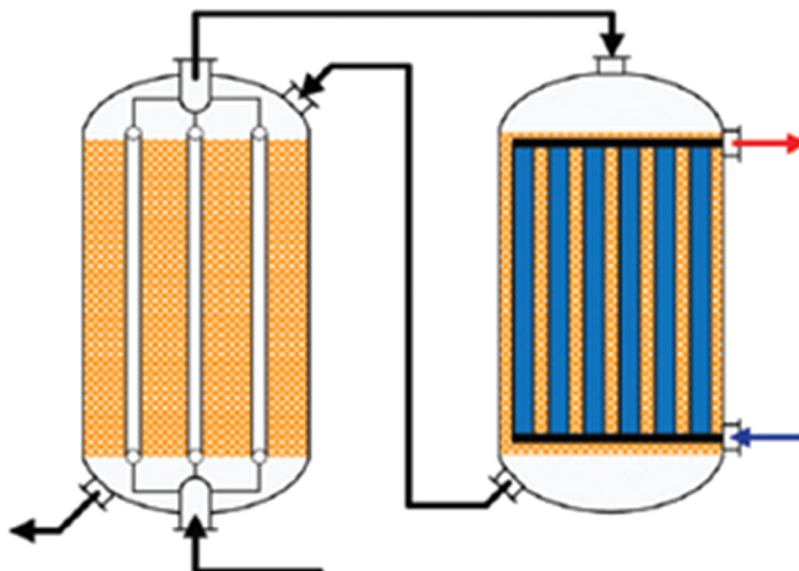


**Figure 4.** MegaMethanol flow scheme.

methanol content. The warm syngas (PREHEATED SYNGAS) is then equally split and fed to two identical boiling water reactors (BWRs), which work in parallel. As in Lurgi single-staged BWR, the heats ( $Q_{BWR1}$  and  $Q_{BWR1}$ ) are recovered producing middle-pressure steam. In the proposed

flowsheet, this step is skipped. The segregated intermediate product flows (streams 5 and 6) are collected and sent to the GCR. The final mixture product (PRODUCTS) is post-processed in the downstream section, which is not reproduced here.

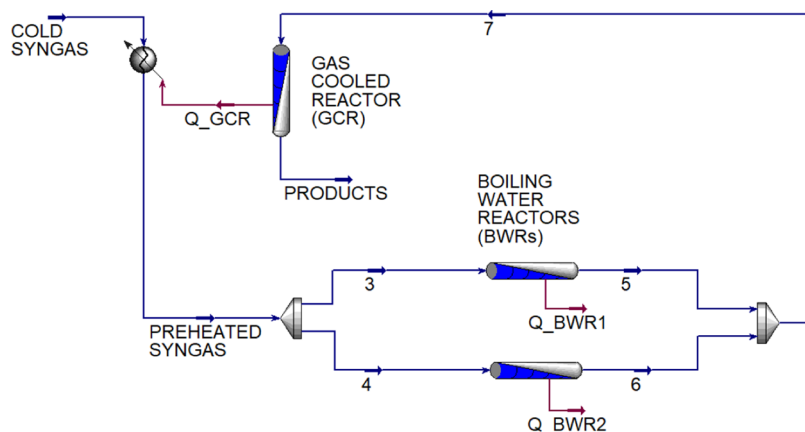


Figure 5. MegaMethanol technology flowsheet in Aspen HYSYS.

The MegaMethanol data are taken from two works by Rahimpour and his collaborators,<sup>78,83</sup> which deal with the same plant and technology. The first paper provides the reactor (GCR and BWRs) specifications, including the feed composition and flow. This work also presents the industrial data for the product stream composition. In the cited work, different plant configurations are analyzed to accomplish process optimization and we focused our efforts on the conventional MegaMethanol simulation, which is the most widespread technology worldwide. Moreover, the plant data refer to the conventional MegaMethanol plant. The second paper defines the temperatures for all of the streams involved in the flowsheet (including the cold syngas feed). Table 15 reports the input (COLD SYNGAS) and reactor specifications (GCR and BWRs). In line with published works,<sup>68,94,95,97</sup> we decided to adopt global average heat transfer coefficients of 60.0 and 200 W/(m<sup>2</sup>·K) for the GCR and BWR respectively.

Table 15. MegaMethanol Plant Specification (Reactors and Cold Syngas Feed)

design specification	gas-cooled (GCR)	water-cooled (BWR) <sup>a</sup>
reactor tube length (m)	10.50	8.40
tubes diameter (cm)	2.54	3.80
number of tubes	3026	5955
temperature along the shell (K)		513
pressure at tube inlet (bar)	76.98	75
pressure at the shell inlet (bar)	72.2	
bed void fraction	0.39	0.39
density of the bed (kg/m <sup>3</sup> )	1140	1140
catalyst particles diameter (mm)	5.70	5.70
average heat transfer coefficient (W/(m <sup>2</sup> ·K))	60.0	250.0
syngas feed (COLD SYNGAS)		
molar flow rate (kmol/h)	30 000	
molar composition		
CO	0.0868	
CO <sub>2</sub>	0.0849	
H <sub>2</sub>	0.6461	
H <sub>2</sub> O	0.0010	
MeOH	0.0037	
CH <sub>4</sub>	0.0947	
N <sub>2</sub>	0.0828	

<sup>a</sup>Design specification refers to the single BWR.

The simulation results are gathered in Table 16, which includes the models' relative errors with respect to the industrial plant data. The measurements are exclusively available for the product stream (PRODUCTS). Intermediate stream composition and temperatures are not provided. As shown, ref-GR is the best-performing kinetics despite the CO<sub>2</sub> and steam contents are not properly predicted. However, it is noticeable that the methanol production and residual hydrogen content are correctly predicted (relative errors <1%), meaning that the ref-GR kinetic is capable of properly predicting the yields of the MegaMethanol technology. Even though the largest deviation is 15%, the outlet stream molar fraction does not present any abnormal deviations as in the case of or-GR: all of the corresponding molar fractions lie in the same order of magnitude and in a very close range. Generally, the relative error is magnified adopting molar fraction. The methanol molar fraction (thus the plant production) is better estimated using ref-GR: both the VBF and or-GR models underestimate such a key parameter (−9 and −65%, respectively). This result confirms previous consideration: or-GR tends to significantly underestimate the methanol productivity, and it would lead to an oversizing of the reactor volume in the design phase. As anticipated, or-GR exhibits the largest deviation on average (20–30%); thus, it does not appear as an appealing kinetic model for the process simulation of the MegaMethanol plant. It is remarkable that this model largely overestimates the final residual CO (it predicts almost a double amount). The VBF kinetic prediction is comparable to those of the ref-GR one; however, it is less accurate and presents larger deviations in estimating the CO<sub>2</sub> and steam contents just like ref-GR but with a wider gap. The predicted GCR outlet temperature is properly predicted by all of the three kinetics, but this result is related to setting proper heat transfer coefficients.

**ICI Technology.** The ICI technology is the easiest to simulate in Aspen HYSYS since the heat removal is through direct quenching. Thus, there is no need for characterizing the heat transfer coefficient. Froment's work provides plant data (industrial case) and the ICI in-house model results for the reactor design (design case).<sup>89</sup> Both conditions have been simulated to compare the kinetic model predictions in two different situations. Figure 6 depicts the technology configurations and the streams name, while Table 17 lists the input data both for the industrial and design cases. The proposed ICI technology consists of five adiabatic packed beds and four quenching side feeds (COOL SHOT). For the industrial case

**Table 16. Results (PRODUCTS Stream) for the Shiraz Company Conventional MegaMethanol Plant as in Rahimpour's Work<sup>83</sup>**

PRODUCTS	industrial data	ref-GR (%)	VBF (%)	or-GR (%)			
T (K)	495	505.2	-2.06	505.2	-2.06	506.3	-2.28
composition (mol/mol)							
CO	0.0251	0.0239	4.85	0.0272	-8.26	0.0743	-196.10
CO <sub>2</sub>	0.0709	0.0819	-15.49	0.0855	-20.55	0.0764	-7.79
H <sub>2</sub>	0.5519	0.5549	-0.55	0.5677	-2.87	0.6096	-10.46
MeOH	0.1040	0.1049	-0.84	0.0943	9.32	0.0359	65.53
H <sub>2</sub> O	0.0234	0.0213	9.09	0.0159	32.14	0.0150	36.07
CH <sub>4</sub>	0.1140	0.1137	0.25	0.1117	1.99	0.1007	11.63
N <sub>2</sub>	0.1107	0.0994	10.18	0.0977	11.75	0.0881	20.43

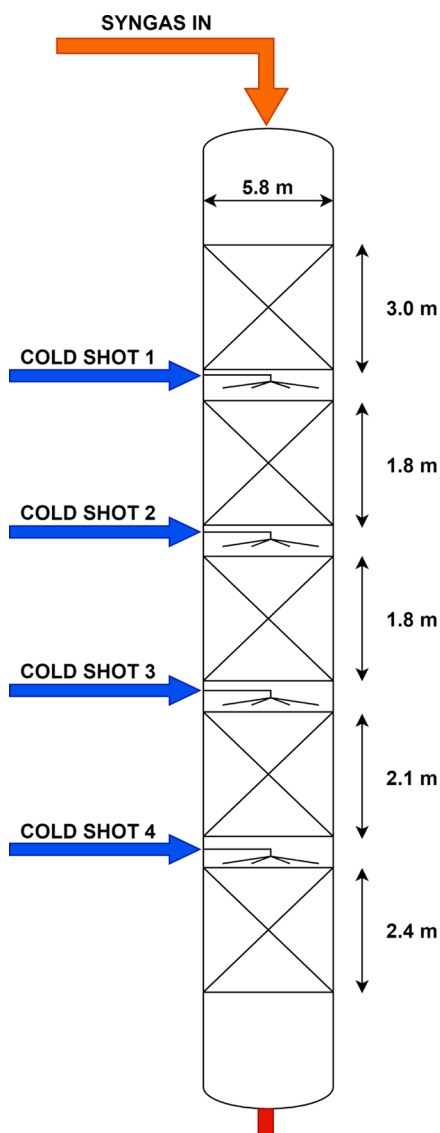


**Figure 6.** ICI reactor case study dimensions and stream names.

and the design one, the compositions of the syngas feed (SYNGAS IN) and the quenching streams are equal while the volumetric flowrates are different depending on the position. The packed bed lengths vary along the reactor, but for both industrial and design cases, they are kept the same. The simulation flowsheet is provided in Figure 7. In the simulation environment, each direct cooling stage is performed as a mixing process assuming it is ideal (i.e., uniform and fast). The

**Table 17. ICI Design and Industrial Case Operating Data**

	design case	industrial case
inlet flow (SYNGAS IN) (Nm <sup>3</sup> /h)	567.1	699.1
inlet pressure (bar)	96.85	90.42
inlet temperature (SYNGAS IN) (K)	505.6	497.7
Cold Shot Flows		
COLD SHOT 1 (Nm <sup>3</sup> /h)	198.9	
COLD SHOT 2 (Nm <sup>3</sup> /h)	236.5	
COLD SHOT 3 (Nm <sup>3</sup> /h)	246.9	
COLD SHOT 4 (Nm <sup>3</sup> /h)	222.1	
COLD SHOT temperature (°C)	83.0	
Cold Shots and Inlet Flow (SYNGAS IN) Molar Composition (mol %)		
MeOH	0.422	0.001
CO <sub>2</sub>	3.581	3.950
CO	4.645	4.200
H <sub>2</sub>	78.50	79.29
H <sub>2</sub> O	0.048	0.001
CH <sub>4</sub>	10.39	10.43
N <sub>2</sub>	2.394	2.128

adiabatic beds are assumed to behave like plug flow reactors (PFR).

Tables 18 and 19 report the simulation results for the design and industrial cases, respectively. The corresponding relative errors estimated with respect to the ICI design and industrial data are reported as percentages in the adjacent column. The results here refer to the VBF model implemented in the reference work.<sup>89</sup> Moreover, industrial measurements for the intermediate and final hydrogen and water flowrates are missing, and only the fifth catalytic bed outlet composition (except hydrogen and steam contents) is available.

From the results (Tables 18 and 19) and charts (Figure 8), it is relevant to notice that kinetic model accuracy is not uniform. The compared kinetic models perform better for design purposes while they exhibit larger deviations in the industrial case. The ref-GR and VBF models are effectively more accurate with regard to the or-GR one in both the proposed case studies. In addition, the ref-GR model is more accurate in predicting the final methanol content rather than or-GR and VBF: for the design case, it shows the lowest relative error, whereas for the industrial case, its accuracy is comparable to the VBF model (relative error ~6% for both and or-GR >10%). Differently from the previous publication, it appears that the or-GR model tends to overestimate the methanol content (Figure 8-2A,2B). This may be misleading since, using the or-GR kinetic, the predicted adiabatic outlet gas temperatures are always the highest (refer to Figure 8-1A,1B), leading to an increment in the reaction rate (i.e., in the

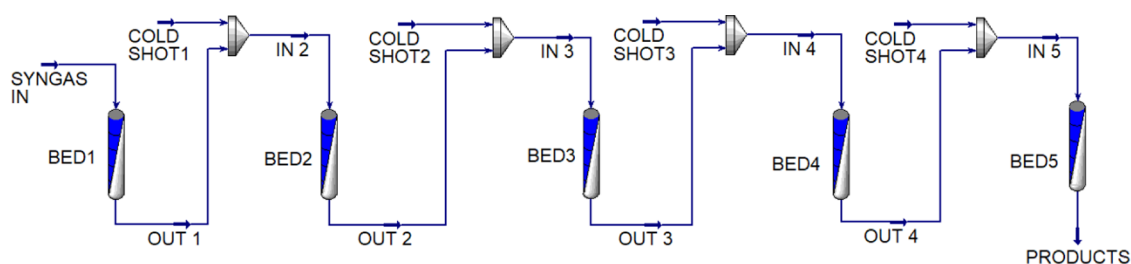


Figure 7. ICI case study flowsheet in Aspen HYSYS.

Table 18. Design Case Results and Comparison (Outlet Temperature and Molar Gas Composition)<sup>a</sup>

catalyst bed	1	2	3	4	5
	Exit T (K)				
ICI design	561.9	555.0	554.0	548.3	545.8
VBF	577.9	564.2	554.9	548.6	544.7
ref-GR	579.9	566.5	557.3	551.2	547.3
or-GR	581.3	567.8	558.5	552.4	548.4
	Exit Gas Composition (mol %) MeOH				
ICI design	2.816	4.016	4.884	5.336	5.712
VBF	3.413	4.315	4.948	5.361	5.616
ref-GR	3.514	4.433	5.08	5.502	5.763
or-GR	3.563	4.48	5.122	5.541	5.800
	Exit Gas Composition (mol %) CO <sub>2</sub>				
ICI design	2.548	2.451	2.289	2.241	2.161
VBF	2.372	2.372	2.342	2.307	2.278
ref-GR	2.301	2.287	2.247	2.204	2.170
or-GR	2.303	2.292	2.253	2.210	2.177
	Exit Gas Composition (mol %) CO				
ICI design	3.695	2.797	2.241	1.914	1.682
VBF	3.378	2.631	2.137	1.830	1.647
ref-GR	3.365	2.617	2.122	1.815	1.643
or-GR	3.322	2.574	2.082	1.777	1.560
	Exit Gas Composition (mol %) H <sub>2</sub>				
ICI design	76.27	75.58	74.98	74.71	74.45
VBF	75.82	75.37	75.03	74.79	74.63
ref-GR	75.7	75.23	74.86	74.61	74.45
or-GR	75.68	75.21	74.85	74.60	74.44
	Exit Gas Composition (mol %) H <sub>2</sub> O				
ICI design	1.254	1.437	1.662	1.742	1.849
VBF	1.472	1.538	1.614	1.679	1.726
ref-GR	1.551	1.631	1.718	1.792	1.844
or-GR	1.552	1.630	1.716	1.788	1.840
	Exit Gas Composition (mol %) CH <sub>4</sub>				
industrial	10.39	11.13	11.31	11.41	11.48
VBF	11.01	11.19	11.32	11.41	11.46
ref-GR	11.03	11.22	11.35	11.44	11.49
or-GR	11.04	11.23	11.36	11.45	11.50
	Exit Gas Composition (mol %) N <sub>2</sub>				
industrial	2.524	2.582	2.623	2.645	2.663
VBF	2.537	2.579	2.609	2.629	2.641
ref-GR	2.541	2.585	2.616	2.636	2.648
or-GR	2.544	2.587	2.618	2.638	2.650

<sup>a</sup>Results provided in the reference paper using the VBF model.<sup>89</sup>

methanol formation in the same catalyst volume). For this reason, or-GR predicts a larger amount of methanol in the product mixture. Furthermore, the comparison between the predictions and the industrial/design data leads to the following considerations: (1) the worst performance for all of the kinetic models is concentrated in the first adiabatic bed, and this may be related to potential mass/heat transfer

limitations around the catalyst particles due to the intensive heat release ( $T > 265$  °C can cause this phenomenon as already discussed in the [Methods](#) section), and (2) the gap among the reference values and the models' predictions is progressively reduced and, in fact, after the second bed, there is a good agreement between ref-GR, VBF, and experimental observations. Despite this, the accuracy in the design case is

Table 19. Industrial Case Results and Comparison

catalyst bed	1	2	3	4	5					
	Exit Temperature (K)									
industrial	560.5	561.3	550.4	544.6	544.7					
VBF	573.1	−2.25%	561.5	−0.04%	552.8	−0.44%	546.7	−0.39%	542.7	0.37%
ref-GR	575.0	−2.59%	563.5	−0.39%	555.0	−0.84%	549.0	−0.81%	545.1	−0.07%
or-GR	576.3	−2.82%	564.7	−0.61%	556.1	−1.04%	550.5	−1.08%	546.1	−0.26%
	Exit Gas Composition (mol %) MeOH									
industrial	NA <sup>a</sup>	NA	NA	NA	4.744					
VBF	3.166	3.872	4.411	4.785	5.026	−5.9%				
ref-GR	3.262	3.983	4.534	4.816	5.062	−6.7%				
or-GR	3.307	4.025	4.572	4.952	5.195	−9.5%				
	Exit Gas Composition (mol %) CO <sub>2</sub>									
industrial	NA	NA	NA	NA	2.838					
VBF	2.527	2.519	2.487	2.332	2.418	14.80%				
ref-GR	2.454	2.435	2.393	2.348	2.612	7.96%				
or-GR	2.457	2.44	2.399	2.355	2.319	18.29%				
	Exit Gas Composition (mol %) CO									
industrial	NA	NA	NA	NA	1.881					
VBF	2.974	2.391	1.972	1.697	1.527	18.82%				
ref-GR	2.967	2.382	1.963	1.688	1.520	19.19%				
or-GR	2.926	2.342	1.925	1.652	1.484	21.11%				
	Exit Gas Composition (mol %) H <sub>2</sub>									
industrial	NA	NA	NA	NA	NA					
VBF	76.31	75.95	75.65	75.43	75.28					
ref-GR	76.19	75.81	75.50	75.26	75.11					
or-GR	76.17	75.80	75.49	75.25	75.10					
	Exit Gas Composition (mol %) H <sub>2</sub> O									
industrial	NA	NA	NA	NA	NA					
VBF	1.674	1.738	1.813	1.880	1.931					
ref-GR	1.755	1.831	1.916	1.991	2.047					
or-GR	1.755	1.829	1.913	1.987	2.043					
	Exit Gas Composition (mol %) CH <sub>4</sub>									
industrial	NA	NA	NA	NA	12.86					
VBF	11.09	11.24	11.35	11.43	11.48	10.73%				
ref-GR	11.11	11.26	11.38	11.46	11.51	10.50%				
or-GR	11.12	11.27	11.38	11.46	11.51	10.50%				
	Exit Gas Composition (mol %) N <sub>2</sub>									
industrial	NA	NA	NA	NA	2.356					
VBF	2.263	2.293	2.316	2.332	2.342	0.59%				
ref-GR	2.267	2.298	2.321	2.337	2.348	0.34%				
or-GR	2.269	2.299	2.323	2.339	2.349	0.30%				

<sup>a</sup>NA—not available.

similar, while, in the industrial case, the ref-GR model has better overall performance. As an instance, it predicts the temperature profile and the methanol content as well as the VBF, but it is more accurate in describing the CO<sub>2</sub> final content, while both VBF and or-GR significantly deviate from experimental data (i.e., relative errors ~15% against 8%). Figure 8-3B depicts an unexpected CO<sub>2</sub> concentration profile. The CO<sub>2</sub> content is monotonically decreasing for four of the catalytic beds, while the last one has a CO<sub>2</sub> content even larger than the first outlet gas mixture. It is not possible to determine whether this plant measurement is an outlier; however, it is remarkable that both ref-GR and VBF predict this low CO<sub>2</sub> increment, whereas the or-GR shows a monotonic reduction in the CO<sub>2</sub> content even for the last adiabatic bed. Hence, it is possible to trust that this anomaly is neither a systematic error in the measurement nor an influential observation since both ref-GR and VBF models predict such a spike in CO<sub>2</sub> content in the final catalytic bed. Concerning the other species, the

accuracy of the models is steady (especially CO, when the relative error stays around 20%), as shown in Figure 8-44A,4B. The hydrogen content is well predicted (Figure 8-5A,5B), while the CO estimates are inaccurate (~20% deviation in the industrial case) independently of the kinetics. More in general, it is possible to state that just considering the final mixture compositions, ref-GR is more reliable than VBF, and it is an effective improvement of the or-GR model regardless of the reactor technology as in Table 20.

## CONCLUSIONS

The present work demonstrated the effectiveness of the methanol reactor process simulation in the Aspen HYSYS simulation suite. Moreover, the performances of three different kinetics have been compared exploiting industrial data for the most worldwide spread methanol technologies such as Lurgi, MegaMethanol, and ICI. We effectively compared the kinetics' performances for each reactor design and adopted the same



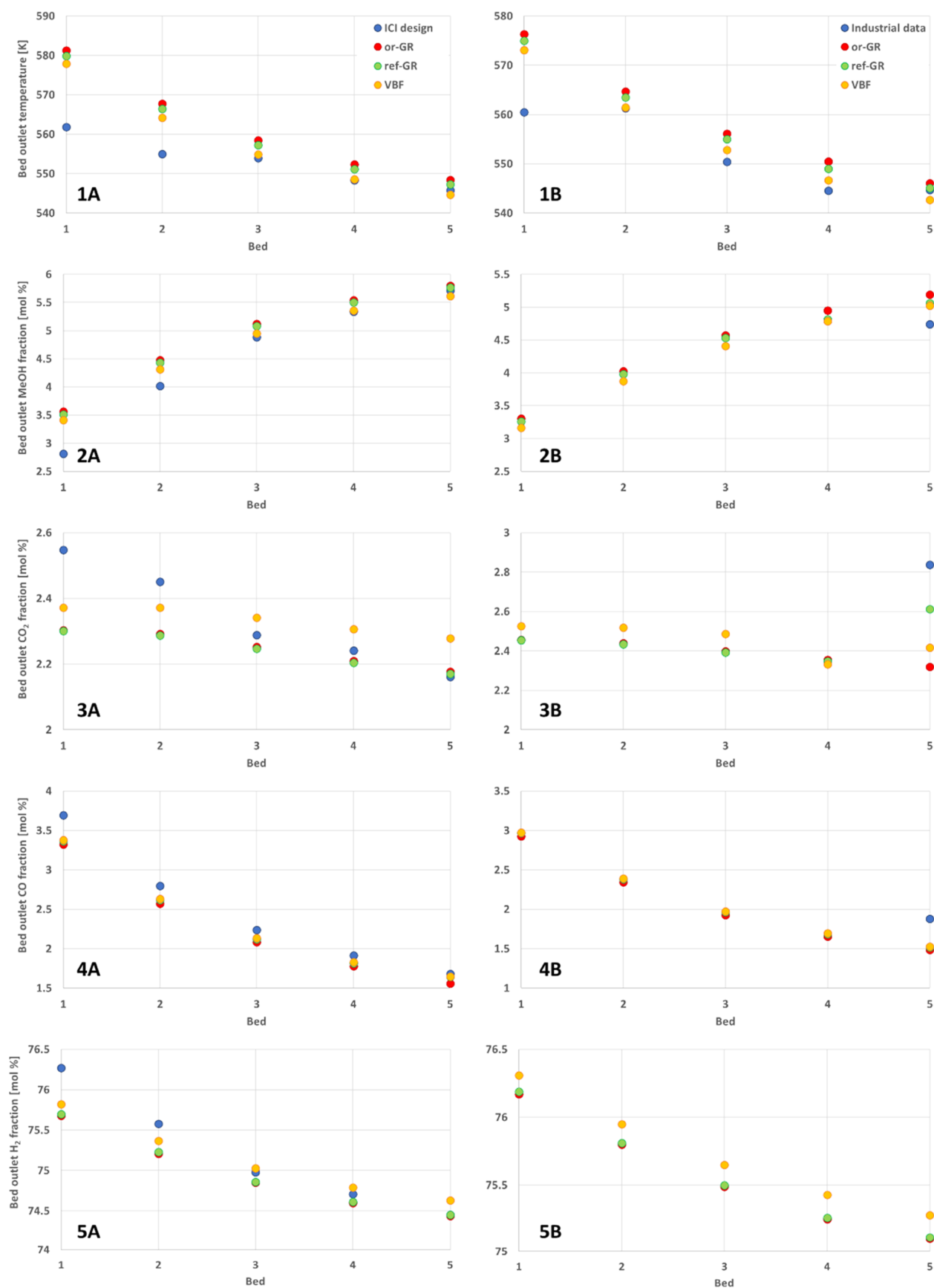


**Figure 8.** ICI results for design (A) and industrial (B) cases: (1) temperature, (2) methanol, (3) CO<sub>2</sub>, (4) CO, and (5) H<sub>2</sub> molar fractions at the adiabatic bed outlet. Industrial/design data are the blue dots, the different kinetics are distinguishable according to the marker color: or-GR (red), ref-GR (green), and VBF (yellow).

Table 20. Resume of Simulation Deviations

	kinetics	deviation in MeOH (%)	deviation in products T (%)	largest dev. (%)	parameter
Lurgi	ref-GR	2.62	-1.37	-8.13	CO mol frac
	VBF	10.30	-0.12	-15.48	CO mol frac
	or-GR	68.96	9.02	-100.90	CO mol frac
MegaMethanol	ref-GR	-0.84	-2.06	9.09	H <sub>2</sub> O mol frac
	VBF	9.32	-2.06	32.14	H <sub>2</sub> O mol frac
	or-GR	65.53	-2.28	-196	CO mol frac
ICI-industrial	ref-GR	-6.70	-0.07	19.19	CO <sub>2</sub> mol frac
	VBF	-5.94	0.37	18.82	CO <sub>2</sub> mol frac
	or-GR	-9.51	-0.26	21.11	CO <sub>2</sub> mol frac
ICI design	ref-GR	-0.89	-0.27	2.32	CO mol frac
	VBF	1.68	0.20	6.65	H <sub>2</sub> O mol frac
	or-GR	-1.54	-0.48	7.25	CO mol frac

integration domain discretization (i.e., the numbers of nodes on the longitudinal axis of the PFR reactor) throughout the simulation. We decided to adopt 100 discretization points. Moreover, material and heat balances are automatically integrated within the Aspen HYSYS V11 ODE solver. Hence, the discrepancies in the predictions can be attributed only to differences in kinetics. Indeed, the kinetics affect both the mixture composition (i.e., the reaction extent and the conversion of the corresponding reactants) and the temperature profile due to the reaction heat released when exothermic reactions occur. Better predictions reflect more accurate and adequate kinetics to describe the system. In our previous work, we refitted or-GR obtaining an updated kinetics, ref-GR. We also showed that ref-GR does not present any abnormal trends in the reaction rate profile under different operating conditions for different feedstocks. In this paper, we aimed at testing our own ref-GR performance not only in describing lab-scale experimental observations. To achieve this target, we needed to use data from industrial-sized plants. The or-GR and VBF are well-established kinetics in the industrial practice while the proposed ref-GR is here adopted to evaluate its predictive capacity and future potential as a suitable kinetic model for industrial applications and purposes. As clearly highlighted in Table 19, ref-GR shows outstanding performances meaning that (1) it is a suitable numerical tool for the methanol sector industry since it presents on average the lowest discrepancies between prediction and data plants, and (2) on the other hand, it effectively removes the shortcoming (i.e., methanol productivity underestimated) in the or-GR kinetics, which were emphasized in previous works. Unfortunately, published industrial data are limited in variability and we are not able to perform the comparison over a wide range of operating conditions, the most likely reason being that industrial methanol plants work in a narrow operating window, which is also where the data are collected. However, we are confident that the four presented industrial case studies are indicative of the accuracy of the ref-GR kinetic. To resume, the ref-GR model better characterizes the methanol converter since it enables us to properly determine the final methanol content regardless of the adopted technology. In the ICI industrial and ICI design case studies, the VBF and ref-GR deviations are comparable, while for the Lurgi and MegaMethanol technologies, the ref-GR deviations are 1 order of magnitude lower. Similar considerations can be provided for the largest deviations. It is remarkable that ref-GR (1) correctly predicts the methanol content with great accuracy (<3% excluding the ICI-industrial example, while under the same hypothesis, VBF

deviation is <10% and or-GR 70% even), (2) the largest deviations do not include the methanol and hydrogen predictions since these are mainly concentrated on the CO<sub>x</sub> and steam molar fractions for all of the three considered kinetics, and (3) outlet temperature is properly determined. Thus, it is proven that ref-GR covers the lack of reliability for industrial purposes. It is more robust and provides accurate outputs with respect to or-GR, and limited to the proposed case studies, it appears more reliable than the VBF model.

## AUTHOR INFORMATION

### Corresponding Author

**Flavio Manenti** – Center for Sustainable Process Engineering Research (SuPER), CMIC Dept. “Giulio Natta”, Politecnico di Milano, 20133 Milan, Italy; [orcid.org/0000-0002-3305-8044](https://orcid.org/0000-0002-3305-8044); Email: [flavio.manenti@polimi.it](mailto:flavio.manenti@polimi.it)

### Authors

**Filippo Bisotti** – Center for Sustainable Process Engineering Research (SuPER), CMIC Dept. “Giulio Natta”, Politecnico di Milano, 20133 Milan, Italy

**Matteo Fedeli** – Center for Sustainable Process Engineering Research (SuPER), CMIC Dept. “Giulio Natta”, Politecnico di Milano, 20133 Milan, Italy

**Kristiano Prifti** – Center for Sustainable Process Engineering Research (SuPER), CMIC Dept. “Giulio Natta”, Politecnico di Milano, 20133 Milan, Italy

**Andrea Galeazzi** – Center for Sustainable Process Engineering Research (SuPER), CMIC Dept. “Giulio Natta”, Politecnico di Milano, 20133 Milan, Italy

**Anna Dell’Angelo** – Center for Sustainable Process Engineering Research (SuPER), CMIC Dept. “Giulio Natta”, Politecnico di Milano, 20133 Milan, Italy

Complete contact information is available at: <https://pubs.acs.org/10.1021/acs.iecr.1c04476>

### Notes

The authors declare no competing financial interest.

## REFERENCES

- (1) Lasala, S.; Chiesa, P.; Privat, R.; Jaubert, J. N. Modeling the Thermodynamics of Fluids Treated by CO<sub>2</sub> Capture Processes with Peng-Robinson + Residual Helmholtz Energy-Based Mixing Rules. *Ind. Eng. Chem. Res.* **2017**, *56*, 2259–2276.
- (2) Lasala, S.; Privat, R.; Jaubert, J. N.; Arpentiner, P. Modelling the Thermodynamics of Air-Component Mixtures (N<sub>2</sub>, O<sub>2</sub> and Ar): Comparison and Performance Analysis of Available Models. *Fluid Phase Equilib.* **2018**, *458*, 278–287.

- (3) Bisotti, F.; Galeazzi, A.; Galatioto, L.; Masserdotti, F.; Bigi, A.; Gritti, P.; Manenti, F. Implementing Robust Thermodynamic Model for Reliable Bubble/Dew Problem Solution in Cryogenic Distillation of Air Separation Units. *Int. J. Thermofluids* **2021**, *10*, No. 100083.
- (4) Pirola, C.; Galli, F.; Manenti, F.; Corbetta, M.; Bianchi, C. L. Simulation and Related Experimental Validation of Acetic Acid/Water Distillation Using p-Xylene as Entrainer. *Ind. Eng. Chem. Res.* **2014**, *53*, 18063–18070.
- (5) Corbetta, M.; Pirola, C.; Galli, F.; Manenti, F. Robust Optimization of the Heteroextractive Distillation Column for the Purification of Water/Acetic Acid Mixtures Using p-Xylene as Entrainer. *Comput. Chem. Eng.* **2016**, *95*, 161–169.
- (6) Manenti, F. Considerations on Nonlinear Model Predictive Control Techniques. *Comput. Chem. Eng.* **2011**, *35*, 2491–2509.
- (7) Marlin, D. S.; Sarron, E.; Sigurbjörnsson, O. Process Advantages of Direct CO<sub>2</sub> to Methanol Synthesis. *Front. Chem.* **2018**, *6*, No. 446.
- (8) Mbatha, S.; Everson, R. C.; Musyoka, N. M.; Langmi, H. W.; Lanzini, A.; Brilman, W. Power-to-Methanol Process: A Review of Electrolysis, Methanol Catalysts, Kinetics, Reactor Designs and Modelling, Process Integration, Optimisation, and Techno-Economics. *Sustainable Energy Fuels* **2021**, *5*, 3490–3569.
- (9) Bildea, C. S.; György, R.; Brunchi, C. C.; Kiss, A. A. Optimal Design of Intensified Processes for DME Synthesis. *Comput. Chem. Eng.* **2017**, *105*, 142–151.
- (10) Luo, H.; Bildea, C. S.; Kiss, A. A. Novel Heat-Pump-Assisted Extractive Distillation for Bioethanol Purification. *Ind. Eng. Chem. Res.* **2015**, *54*, 2208–2213.
- (11) Dimian, A. C.; Kiss, A. A. Enhancing the Separation Efficiency in Acetic Acid Manufacturing by Methanol Carbonylation. *Chem. Eng. Technol.* **2021**, *44*, 1792–1802.
- (12) Simon, L. L.; Kiss, A. A.; Cornevin, J.; Gani, R. Process Engineering Advances in Pharmaceutical and Chemical Industries: Digital Process Design, Advanced Rectification, and Continuous Filtration. *Curr. Opin. Chem. Eng.* **2019**, *25*, 114–121.
- (13) Bisotti, F.; Fedeli, M.; Prifti, K.; Galeazzi, A.; Angelo, A. D.; Barbieri, M.; Pirola, C.; Bozzano, G.; Manenti, F. Century of Technology Trends in Methanol Synthesis: Any Need for Kinetics Refitting? *Ind. Eng. Chem. Res.* **2021**, 16032.
- (14) Bozzano, G.; Manenti, F. Efficient Methanol Synthesis: Perspectives, Technologies and Optimization Strategies. *Prog. Energy Combust. Sci.* **2016**, *56*, 71–105.
- (15) Dieterich, V.; Buttler, A.; Hanel, A.; Spliethoff, H.; Fendt, S. Power-to-Liquid via Synthesis of Methanol, DME or Fischer-Tropsch-Fuels: A Review. *Energy Environ. Sci.* **2020**, *13*, 3207–3252.
- (16) Pirola, C.; Bozzano, G.; Manenti, F. In *Fossil or Renewable Sources for Methanol Production?*; Basile, A.; Dalena, F. B. T.-M., Eds.; Elsevier, 2018; Chapter 3, pp 53–93.
- (17) Bains, P.; Psarras, P.; Wilcox, J. CO<sub>2</sub> Capture from the Industry Sector. *Prog. Energy Combust. Sci.* **2017**, *63*, 146–172.
- (18) Al Baroudi, H.; Awoyomi, A.; Patchigolla, K.; Jonnalagadda, K.; Anthony, E. J. A Review of Large-Scale CO<sub>2</sub> Shipping and Marine Emissions Management for Carbon Capture, Utilisation and Storage. *Appl. Energy* **2021**, *287*, No. 116510.
- (19) Yu, K. M. K.; Curcic, I.; Gabriel, J.; Tsang, S. C. E. Recent Advances in CO<sub>2</sub> Capture and Utilization. *ChemSusChem* **2008**, *1*, 893–899.
- (20) Al-Mamoori, A.; Krishnamurthy, A.; Rownaghi, A. A.; Rezaei, F. Carbon Capture and Utilization Update. *Energy Technol.* **2017**, *5*, 834–849.
- (21) Marocco Stuardi, F.; MacPherson, F.; Leclaire, J. Integrated CO<sub>2</sub> Capture and Utilization: A Priority Research Direction. *Curr. Opin. Green Sustainable Chem.* **2019**, *16*, 71–76.
- (22) Fernández, J. R.; Garcia, S.; Sanz-Pérez, E. S. CO<sub>2</sub> Capture and Utilization Editorial. *Ind. Eng. Chem. Res.* **2020**, *59*, 6767–6772.
- (23) Roh, K.; Lim, H.; Chung, W.; Oh, J.; Yoo, H.; Al-Hunaidy, A. S.; Imran, H.; Lee, J. H. Sustainability Analysis of CO<sub>2</sub> Capture and Utilization Processes Using a Computer-Aided Tool. *J. CO<sub>2</sub> Util.* **2018**, *26*, 60–69.
- (24) Marshall, M. From Pollution to Solution. *New Sci.* **2018**, *237*, 34–37.
- (25) Ostadi, M.; Paso, K. G.; Rodriguez-Fabia, S.; Øi, L. E.; Manenti, F.; Hillestad, M. Process Integration of Green Hydrogen: Decarbonization of Chemical Industries. *Energies* **2020**, *13*, No. 4859.
- (26) Kaiser, P.; Unde, R. B.; Kern, C.; Jess, A. Production of Liquid Hydrocarbons with CO<sub>2</sub> as Carbon Source Based on Reverse Water-Gas Shift and Fischer-Tropsch Synthesis. *Chem.-Ing.-Tech.* **2013**, *85*, 489–499.
- (27) Hillestad, M.; Ostadi, M.; Alamo Serrano, G. D.; Rytter, E.; Austbø, B.; Pharoah, J. G.; Burheim, O. S. Improving Carbon Efficiency and Profitability of the Biomass to Liquid Process with Hydrogen from Renewable Power. *Fuel* **2018**, *234*, 1431–1451.
- (28) Pérez-Fortes, M.; Moya, J. A.; Vatopoulos, K.; Tzimas, E. CO<sub>2</sub> Capture and Utilization in Cement and Iron and Steel Industries. *Energy Procedia* **2014**, *63*, 6534–6543.
- (29) Mennicken, L.; Janz, A.; Roth, S. The German R&D Program for CO<sub>2</sub> Utilization—Innovations for a Green Economy. *Environ. Sci. Pollut. Res.* **2016**, *23*, 11386–11392.
- (30) Kim, M.; Kim, K.; Kim, T.-h.; Kim, J. Economic and Environmental Benefit Analysis of a Renewable Energy Supply System Integrated with Carbon Capture and Utilization Framework. *Chem. Eng. Res. Des.* **2019**, *147*, 200–213.
- (31) Wich, T.; Lueke, W.; Deerberg, G.; Oles, M. Carbon2Chem-CCU as a Step Toward a Circular Economy. *Front. Energy Res.* **2020**, *7*, No. 162.
- (32) Villa, P.; Forzatti, P.; Buzzi-Ferraris, G.; Garone, G.; Pasquon, I. Synthesis of Alcohols from Carbon Oxides and Hydrogen. 1. Kinetics of the Low-Pressure Methanol Synthesis. *Ind. Eng. Chem. Process Des. Dev.* **1985**, *24*, 12–19.
- (33) Klier, K.; Chatikavanij, V.; Herman, R. G.; Simmons, G. W. Catalytic Synthesis of Methanol from COH<sub>2</sub>: IV. The Effects of Carbon Dioxide. *J. Catal.* **1982**, *74*, 343–360.
- (34) Seidel, C.; Jörke, A.; Vollbrecht, B.; Seidel-Morgenstern, A.; Kienle, A. Kinetic Modeling of Methanol Synthesis from Renewable Resources. *Chem. Eng. Sci.* **2018**, *175*, 130–138.
- (35) Park, N.; Park, M.-J.; Lee, Y.-J.; Ha, K.-S.; Jun, K.-W. Kinetic Modeling of Methanol Synthesis over Commercial Catalysts Based on Three-Site Adsorption. *Fuel Process. Technol.* **2014**, *125*, 139–147.
- (36) Lim, H.-W.; Park, M.-J.; Kang, S.-H.; Chae, H.-J.; Bae, J. W.; Jun, K.-W. Modeling of the Kinetics for Methanol Synthesis Using Cu/ZnO/Al<sub>2</sub>O<sub>3</sub>/ZrO<sub>2</sub> Catalyst: Influence of Carbon Dioxide during Hydrogenation. *Ind. Eng. Chem. Res.* **2009**, *48*, 10448–10455.
- (37) Chinchin, G. C.; Denny, P. J.; Jennings, J. R.; Spencer, M. S.; Waugh, K. C. Synthesis of Methanol. Part 1. Catalysts and Kinetics. *Appl. Catal.* **1988**, *36*, 1–65.
- (38) Guil-López, R.; Mota, N.; Llorente, J.; Millán, E.; Pawelec, B.; Fierro, J. L. G.; Navarro, R. M. Methanol Synthesis from CO<sub>2</sub>: A Review of the Latest Developments in Heterogeneous Catalysis. *Materials* **2019**, *12*, No. 3902.
- (39) Laudenschleger, D.; Ruland, H.; Muhler, M. Identifying the Nature of the Active Sites in Methanol Synthesis over Cu/ZnO/Al<sub>2</sub>O<sub>3</sub> Catalysts. *Nat. Commun.* **2020**, *11*, No. 3898.
- (40) Stolar, T.; Prašnikar, A.; Martínez, V.; Karadeniz, B.; Bjelić, A.; Mali, G.; Friščić, T.; Likozar, B.; Užarević, K. Scalable Mechanochemical Amorphization of Bimetallic Cu-Zn MOF-74 Catalyst for Selective CO<sub>2</sub> Reduction Reaction to Methanol. *ACS Appl. Mater. Interfaces* **2021**, *13*, 3070–3077.
- (41) Pavlišić, A.; Huš, M.; Prašnikar, A.; Likozar, B. Multiscale Modelling of CO<sub>2</sub> Reduction to Methanol over Industrial Cu/ZnO/Al<sub>2</sub>O<sub>3</sub> Heterogeneous Catalyst: Linking Ab Initio Surface Reaction Kinetics with Reactor Fluid Dynamics. *J. Cleaner Prod.* **2020**, *275*, No. 122958.
- (42) Prašnikar, A.; Jurković, D. L.; Likozar, B. Reaction Path Analysis of CO<sub>2</sub> Reduction to Methanol through Multisite Microkinetic Modelling over Cu/ZnO/Al<sub>2</sub>O<sub>3</sub> Catalysts. *Appl. Catal., B* **2021**, *292*, No. 120190.
- (43) Lacerda de Oliveira Campos, B.; Herrera Delgado, K.; Pitter, S.; Sauer, J. Development of Consistent Kinetic Models Derived from a

Microkinetic Model of the Methanol Synthesis. *Ind. Eng. Chem. Res.* **2021**, *15074*.

(44) Slotboom, Y.; Bos, M. J.; Pieper, J.; Vrieswijk, V.; Likozar, B.; Kersten, S. R. A.; Brilman, D. W. F. Critical Assessment of Steady-State Kinetic Models for the Synthesis of Methanol over an Industrial Cu/ZnO/Al<sub>2</sub>O<sub>3</sub> Catalyst. *Chem. Eng. J.* **2020**, *389*, No. 124181.

(45) Moulijn, J. A. et al. *Chemical Process Technology*; Wiley, 2013; Vol. 51.

(46) Weissermel, K.; Arpe, H. *Industrial Organic Chemistry*; John Wiley & Sons, 2003.

(47) Previtali, D.; Longhi, M.; Galli, F.; Di Michele, A.; Manenti, F.; Signoretto, M.; Menegazzo, F.; Pirola, C. Low Pressure Conversion of CO<sub>2</sub> to Methanol over Cu/Zn/Al Catalysts. The Effect of Mg, Ca and Sr as Basic Promoters. *Fuel* **2020**, *274*, No. 117804.

(48) McNeil, M. A.; Schack, C. J.; Rinker, R. G. Methanol Synthesis from Hydrogen, Carbon Monoxide and Carbon Dioxide over a CuO/ZnO/Al<sub>2</sub>O<sub>3</sub> Catalyst: II. Development of a Phenomenological Rate Expression. *Appl. Catal.* **1989**, *50*, 265–285.

(49) Ma, H.; Ying, W.; Fang, D. Study on Methanol Synthesis from Coal-Based Syngas. *J. Coal Sci. Eng.* **2009**, *15*, 98–103.

(50) Takagawa, M.; Ohsugi, M. Study on Reaction Rates for Methanol Synthesis from Carbon Monoxide, Carbon Dioxide, and Hydrogen. *J. Catal.* **1987**, *107*, 161–172.

(51) Graaf, G. H.; Stamhuis, E. J.; Beenackers, A. A. C. M. Kinetics of Low-Pressure Methanol Synthesis. *Chem. Eng. Sci.* **1988**, *43*, 3185–3195.

(52) Nestler, F.; Schütze, A. R.; Ouda, M.; Hadrach, M. J.; Schaadt, A.; Bajohr, S.; Kolb, T. Kinetic Modelling of Methanol Synthesis over Commercial Catalysts: A Critical Assessment. *Chem. Eng. J.* **2020**, *394*, No. 124881.

(53) Skrzypek, J.; Lachowska, M.; Moroz, H. Kinetics of Methanol Synthesis over Commercial Copper/Zinc Oxide/Alumina Catalysts. *Chem. Eng. Sci.* **1991**, *46*, 2809–2813.

(54) Askgaard, T. S.; Norskov, J. K.; Ovesen, C. V.; Stoltze, P. A Kinetic Model of Methanol Synthesis. *J. Catal.* **1995**, *156*, 229–242.

(55) Vanden Bussche, K. M.; Froment, G. F. A Steady-State Kinetic Model for Methanol Synthesis and the Water Gas Shift Reaction on a Commercial Cu/ZnO/Al<sub>2</sub>O<sub>3</sub> Catalyst. *J. Catal.* **1996**, *161*, 1–10.

(56) Kubota, T.; Hayakawa, I.; Mabuse, H.; Mori, K.; Ushikoshi, K.; Watanabe, T.; Saito, M. Kinetic Study of Methanol Synthesis from Carbon Dioxide and Hydrogen. *Appl. Organomet. Chem.* **2001**, *15*, 121–126.

(57) Buzzi-Ferraris, G.; Manenti, F. Data Interpretation and Correlation. *Kirk-Othmer Encyclopedia of Chemical Technology*; Wiley: New York, 2011.

(58) Buzzi-Ferraris, G.; Manenti, F. *Interpolation and Regression Models for the Chemical Engineers: Solving Numerical Problems*; Wiley-VCH: Weinheim, Germany, 2010.

(59) Buzzi-Ferraris, G.; Manenti, F. *Nonlinear Systems and Optimization for the Chemical Engineer: Solving Numerical Problems*; John Wiley & Sons, Inc., 2013.

(60) Manenti, F.; Buzzi-Ferraris, G. Criteria for Outliers Detection in Nonlinear Regression Problems. In *19 European Symposium on Computer Aided Process Engineering*; Jezowski, J.; Thullie, J., Eds.; Computer Aided Chemical Engineering; Elsevier, 2009; Vol. 26, pp 913–917.

(61) Lange, J. P. Methanol Synthesis: A Short Review of Technology Improvements. *Catal. Today* **2001**, *64*, 3–8.

(62) Tijm, P. J. A.; Waller, F. J.; Brown, D. M. Methanol Technology Developments for the New Millennium. *Appl. Catal., A* **2001**, *221*, 275–282.

(63) Westerterp, K. R. New Methanol Processes. In *Energy Efficiency in Process Technology*; Pilavachi, P. A., Ed.; Springer: Netherlands, 1993; pp 1142–1153.

(64) Wernicke, H.-J.; Plass, L.; Schmidt, F. Methanol Generation. In *Methanol: The Basic Chemical and Energy Feedstock of the Future*; Bertau, M.; Offermanns, H.; Plass, L.; Schmidt, F.; Wernicke, H.-J., Eds.; Springer: Berlin, Heidelberg, 2014; pp 51–301.

(65) Graaf, G. H.; Beenackers, A. A. C. M. Comparison of Two-Phase and Three-Phase Methanol Synthesis Processes. *Chem. Eng. Process.* **1996**, *35*, 413–427.

(66) Hansen, J. B.; Højlund Nielsen, P. E. Methanol Synthesis. *Handbook of Heterogeneous Catalysis*; John Wiley & Sons, Inc., 2008; pp 2920–2949.

(67) Ott, J.; Gronemann, V.; Pontzen, F.; Fiedler, E.; Grossman, G.; Burkhard Kersebohm, K.; Weiss, G.; Witte, C. Methanol - An Industrial Review. *Ullmann's Encyclopedia of Industrial Chemistry*; Wiley-VCH Verlag GmbH & Co. KGaA, 2012.

(68) Cui, X.; Kær, S. K. A Comparative Study on Three Reactor Types for Methanol Synthesis from Syngas and CO<sub>2</sub>. *Chem. Eng. J.* **2020**, *393*, No. 124632.

(69) Heydorn, E. C.; Diamond, B. W.; Lilly, R. D. *Commercial-Scale Demonstration of the Liquid Phase Methanol (LPMEOH) Process*; Air Products Liquid Phase Conversion Company, L.P., 2003.

(70) Eigenberger, G.; Werther, J.; Schoenfelder, H.; Beenackers, A. A. C. M.; St Matros, Y.; Bunimovich, G. A.; Donati, G.; Habashi, N.; Miracca, I.; Sanfilippo, D. Reaction Engineering. *Handbook of Heterogeneous Catalysis*; John Wiley & Sons, Inc., 1997; pp 1399–1487.

(71) Palma, V.; Meloni, E.; Ruocco, C.; Martino, M.; Ricca, A. In *State of the Art of Conventional Reactors for Methanol Production*; Basile, A.; Dalena, F. B. T.-M., Eds.; Elsevier, 2018; Chapter 2, pp 29–51.

(72) Cybulski, A. Liquid-Phase Methanol Synthesis: Catalysts, Mechanism, Kinetics, Chemical Equilibria, Vapor–Liquid Equilibria, and Modeling—a Review. *Catal. Rev.* **1994**, *36*, 557–615.

(73) Riaz, A.; Zahedi, G.; Klemeš, J. J. A Review of Cleaner Production Methods for the Manufacture of Methanol. *J. Cleaner Prod.* **2013**, *57*, 19–37.

(74) Hirotsani, K.; Nakamura, H.; Shoji, K. Optimum Catalytic Reactor Design for Methanol Synthesis with TEC MRF-Z Reactor. *Catal. Surv. Jpn.* **1998**, *2*, 99–106.

(75) Lembeck, M. Linde isothermal reactor for methanol synthesis. *Linde Ber. Tech. Wiss.* **1986**, *58*, No. DE-86-007253.

(76) Haid, J.; Koss, U. Lurgi's Mega-Methanol Technology Opens the Door for a New Era in down-Stream Applications. *Natural Gas Conversion VI*; Studies in Surface Science and Catalysis; Elsevier Science B.V., 2001; Vol. 136, pp 399–404.

(77) Wurzel, T. Lurgi Megamethanol Technology - Delivering the Building Blocks for the Future Fuel and Monomer Demand. *Oil, Gas* **2007**, *33*, 92–96.

(78) Keramat, F.; Mirvakili, A.; Shariati, A.; Rahimpour, M. R. Investigation of Anti-Condensation Strategies in the Methanol Synthesis Reactor Using Computational Fluid Dynamics. *Korean J. Chem. Eng.* **2021**, *38*, 2020–2033.

(79) Heydorn, E. C.; Stein, V. E.; Tijm, P. J. A.; Street, B. T.; Kornosky, R. M. In *Liquid Phase Methanol (LPMEOHTM) Project Operational Experience*, Presented at the Gasification Technology Council Meeting in San Francisco on October 4–7, 1998.

(80) Porter, R. C.; Mills, O. Book Review: Commercial-Scale Demonstration of the Liquid Phase Methanol (LPMEOH<sup>TM</sup>) Process. *Energy Explor. Exploit.* **1999**, *17*, 640–641.

(81) Manenti, F.; Cieri, S.; Restelli, M. Considerations on the Steady-State Modeling of Methanol Synthesis Fixed-Bed Reactor. *Chem. Eng. Sci.* **2011**, *66*, 152–162.

(82) Leonzio, G. Mathematical Modeling of a Methanol Reactor by Using Different Kinetic Models. *J. Ind. Eng. Chem.* **2020**, *85*, 130–140.

(83) Rahmatmand, B.; Rahimpour, M. R.; Keshavarz, P. Introducing a Novel Process to Enhance the Syngas Conversion to Methanol over Cu/ZnO/Al<sub>2</sub>O<sub>3</sub> Catalyst. *Fuel Process. Technol.* **2019**, *193*, 159–179.

(84) Wurzel, T. In *Lurgi Megamethanol Technology—Delivering the Building Blocks for the Future Fuel and Monomer Demand*, DGMK/SCI Conference: Synthesis Gas Chemistry, Dresden, Germany, 2006.

(85) Walid, B. A. B. T.; Hassiba, B.; Boumediene, H.; Weifeng, S. Improved Design of the Lurgi Reactor for Methanol Synthesis Industry. *Chem. Eng. Technol.* **2018**, *41*, 2043–2052.

(86) Mäyrä, O.; Leiviskä, K. Modeling in Methanol Synthesis. In *Methanol*; Basile, A.; Dalena, F., Eds.; Elsevier, 2018; Chapter 17, pp 475–492.

(87) Chen, L.; Jiang, Q.; Song, Z.; Posarac, D. Optimization of Methanol Yield from a Lurgi Reactor. *Chem. Eng. Technol.* **2011**, *34*, 817–822.

(88) Alarifi, A.; Liu, Z.; Erenay, F. S.; Elkamel, A.; Croiset, E. Dynamic Optimization of Lurgi Type Methanol Reactor Using Hybrid GA-GPS Algorithm: The Optimal Shell Temperature Trajectory and Carbon Dioxide Utilization. *Ind. Eng. Chem. Res.* **2016**, *55*, 1164–1173.

(89) Al-Fadli, A. M.; Soliman, M. A.; Froment, G. F. Steady State Simulation of a Multi-Bed Adiabatic Reactor for Methanol Production. *J. King Saud Univ.—Eng. Sci.* **1995**, *7*, 101–132.

(90) Mirvakili, A.; Chahibakhsh, S.; Ebrahimzadehsarvestani, M.; Soroush, E.; Rahimpour, M. R. Modeling and Assessment of Novel Configurations to Enhance Methanol Production in Industrial Mega-Methanol Synthesis Plant. *J. Taiwan Inst. Chem. Eng.* **2019**, *104*, 40–53.

(91) Rezaie, N.; Jahanmiri, A.; Moghtaderi, B.; Rahimpour, M. R. A Comparison of Homogeneous and Heterogeneous Dynamic Models for Industrial Methanol Reactors in the Presence of Catalyst Deactivation. *Chem. Eng. Process.* **2005**, *44*, 911–921.

(92) Manenti, F.; Cieri, S.; Restelli, M.; Bozzano, G. Dynamic Modeling of the Methanol Synthesis Fixed-Bed Reactor. *Comput. Chem. Eng.* **2013**, *48*, 325–334.

(93) Meyer, J. J.; Tan, P.; Apfelbacher, A.; Daschner, R.; Hornung, A. Modeling of a Methanol Synthesis Reactor for Storage of Renewable Energy and Conversion of CO<sub>2</sub> - Comparison of Two Kinetic Models. *Chem. Eng. Technol.* **2016**, *39*, 233–245.

(94) De María, R.; Díaz, I.; Rodríguez, M.; Sáiz, A. Industrial Methanol from Syngas: Kinetic Study and Process Simulation. *Int. J. Chem. React. Eng.* **2013**, *11*, 469–477.

(95) Luyben, W. L. Design and Control of a Methanol Reactor/Column Process. *Ind. Eng. Chem. Res.* **2010**, *49*, 6150–6163.

(96) Rafiee, A. Optimal Design Issues of a Methanol Synthesis Reactor from CO<sub>2</sub> Hydrogenation. *Chem. Eng. Technol.* **2020**, *43*, 2092–2099.

(97) Bøhn, K. Design Configurations of the Methanol Synthesis Loop. *Chemical Engineering and Biotechnology*; Norwegian University of Science and Technology, 2011.

## Recommended by ACS

### A Unified Reactor Network Synthesis Framework for Simultaneous Consideration of Batch and Continuous-Flow Reactor Alternatives

Joseph G. Costandy, Michael Baldea, *et al.*

MAY 06, 2021

INDUSTRIAL & ENGINEERING CHEMISTRY RESEARCH

READ 

### Identification of Key Transport Phenomena in High-Temperature Reactors: Flow and Heat Transfer Characteristics

Georg Liesche and Kai Sundmacher

OCTOBER 25, 2018

INDUSTRIAL & ENGINEERING CHEMISTRY RESEARCH

READ 

### Identification of Optimal Catalyst Distributions in Heat-Exchanger Reactors

Sunjeev Venkateswaran, Costas Kravaris, *et al.*

MARCH 08, 2020

INDUSTRIAL & ENGINEERING CHEMISTRY RESEARCH

READ 

### From Laboratory to Industrial Operation: Model-Based Digital Design and Optimization of Fixed-Bed Catalytic Reactors

Stepan Spatenka, Alejandro Cano, *et al.*

JUNE 12, 2019

INDUSTRIAL & ENGINEERING CHEMISTRY RESEARCH

READ 

Get More Suggestions >